

Synthesis of 7-Azaindoles by Chichibabin Cyclization:
Reversible Base-Mediated Dimerization of 3-Picolines

Yun Ma, Sean Breslin, Ivan Keresztes, Emil Lobkovsky and David B. Collum*†

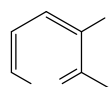
Contribution from the Department of Chemistry and Chemical Biology
Baker Laboratory, Cornell University, Ithaca, New York 14853-1301

Supporting Information

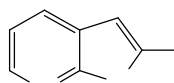
I	¹ H and ¹³ C NMR spectra of 2 in DMSO- <i>d</i> ₆ .	S5
II	¹⁹ F NMR spectra of 1 with LDA in neat THF showing reaction to form 5 .	S6
III	⁶ Li and ¹⁹ F NMR spectra of 1 with LDA in neat THF showing reaction to form 5 .	S7
IV	⁶ Li NMR spectra of 1 with [⁶ Li, ¹⁵ N]LDA in neat THF after aging to form 5 .	S8
V	¹ H NMR and ¹³ C NMR spectra of 1 with LDA in neat THF- <i>d</i> ₈ showing reaction to form 5 .	S9
VI	¹ H NMR spectra of 1 with LDA in neat THF- <i>d</i> ₈ showing reaction to form 5 . Only aromatic and vinylic regions are displayed.	S10
VII	[¹ H, ¹ H]COSY spectrum of 1 with LDA in neat THF- <i>d</i> ₈ showing reaction to form 5 .	S11
VIII	[¹ H, ¹³ C]HMBC spectrum of 1 with LDA in neat THF- <i>d</i> ₈ showing reaction to form 5 .	S12
IX	<i>J</i> { ¹ H, ¹⁹ F}resolved spectrum of 1 with LDA in neat THF- <i>d</i> ₈ showing reaction to form 5 .	S13
X	¹⁹ F NMR spectra of 5 in neat THF- <i>d</i> ₈ after H ₂ O/THF quench to form 7 .	S14
XI	[¹ H, ¹ H]COSY spectrum of 7 in neat THF- <i>d</i> ₈ .	S15
XII	[¹ H, ¹³ C]HSQC spectrum of 7 in neat THF- <i>d</i> ₈ .	S16
XIII	[¹ H, ¹³ C]HMBC spectrum of 7 in neat THF- <i>d</i> ₈ .	S17
XIV	¹ H NMR spectra of 8a and 8b in acetone- <i>d</i> ₆ .	S18

XV	$^1\text{H}, ^{13}\text{C}$]HMBC spectrum of 8a and 8b in acetone- d_6 .	S19
XVI	$^1\text{H}, ^{13}\text{C}$]HMBC spectrum of 8a and 8b in acetone- d_6 with zoom on methyl region.	S20
XVII	^1H and ^{13}C NMR spectra of 9 in acetone- d_6 .	S21
XVIII	^1H and ^{13}C NMR spectra of 10 in acetone- d_6 .	S22
XIX	$^1\text{H}, ^1\text{H}$]COSY spectrum of 10 in acetone- d_6 .	S23
XX	$^1\text{H}, ^{13}\text{C}$]HSQC spectrum of 10 in acetone- d_6 .	S24
XXI	$^1\text{H}, ^{13}\text{C}$]HMBC spectrum of 10 in acetone- d_6 .	S25
XXII	^{19}F NMR spectra of 1 with LDA in neat THF showing reaction to form 5 and 13 .	S26
XXIII	^1H and ^{13}C NMR spectra of 23 in neat THF- d_8 .	S27
XXIV	$^1\text{H}^1\text{H}$]COSY spectrum of 23 in neat THF- d_8 .	S28
XXV	$^1\text{H}, ^{13}\text{C}$]HMBC spectrum of 23 in neat THF- d_8 .	S29
XXVI	$^1\text{H}, ^{13}\text{C}$]HSQC spectrum of 23 in neat THF- d_8 .	S30
XXVII	Mass spectra of 9 and 9-d_5 .	S31
XXVIII	Mass spectra of 9 , 9-d_2 , 9-d_3 , and 9-d_5 with zoom on M+ peak region.	S32
XXIX	^6Li NMR spectra of 6 in neat THF showing reaction to form 18 , 19 and 14 recorded at -90 °C.	S33
XXX	^6Li NMR spectra of 6 in neat THF showing reaction to form 17 , 18 , and 14 recorded at -50 and -40 °C.	S34
XXXI	^6Li NMR spectra of [$^6\text{Li}, ^{15}\text{N}$]LDA plus PhCN in neat THF.	S35
XXXII	^6Li NMR spectra of 6 and [^6Li]LDA in neat THF with the addition of 1 .	S36
XXXIII	^{19}F NMR spectra of 6 with LDA in neat THF with the addition of 1 at -40 °C.	S37

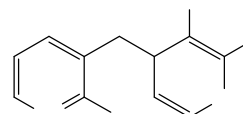
XXXIV	Plot of k_{obsd} vs [THF] in pentane for the deprotonation of 1 by LDA.	S38
XXXV	Plot of k_{obsd} vs [THF] in 2,2,5,5-Me ₄ THF for the deprotonation of 1 by LDA.	S39
XXXVI	Plot of k_{obsd} vs [LDA] in THF/pentane for the deprotonation of 1 by LDA.	S40
XXXVII	Plot of k_{obsd} vs [THF] in pentane for the deprotonation of 1 by LDA as determined following product formation via in situ IR.	S41
XXXVIII	Plot of k_{obsd} vs [LDA] in THF for the deprotonation of 1 by LDA as determined following product formation via in situ IR.	S42
XXXIX	Plot of k_{obsd} vs [LDA] in THF/pentane for the lithiation of PhCN by LDA as determined following product formation via in situ IR.	S43
XL	Plot of k_{obsd} vs [THF] in pentane for the lithiation of PhCN by LDA as determined following product formation via in situ IR.	S44
XLI	X-Ray structure of compound 9 .	S45



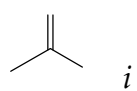
1



2

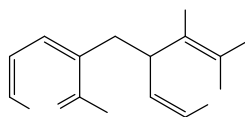


5

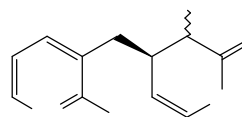


6

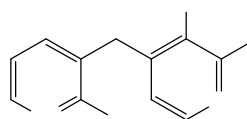
i



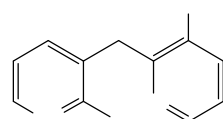
7



8



9



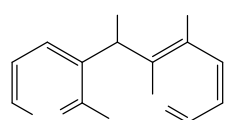
10



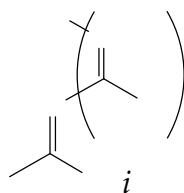
11

i

i



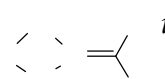
13



14

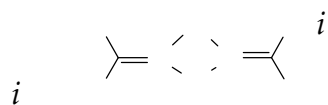
i

i



18

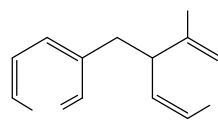
i



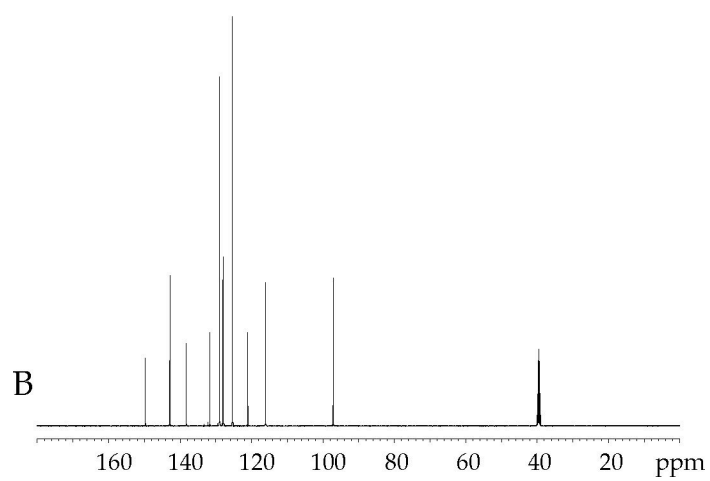
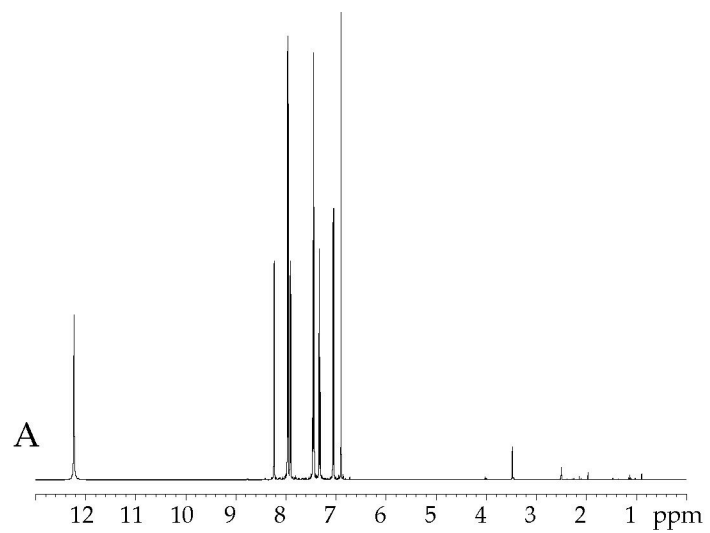
19

i

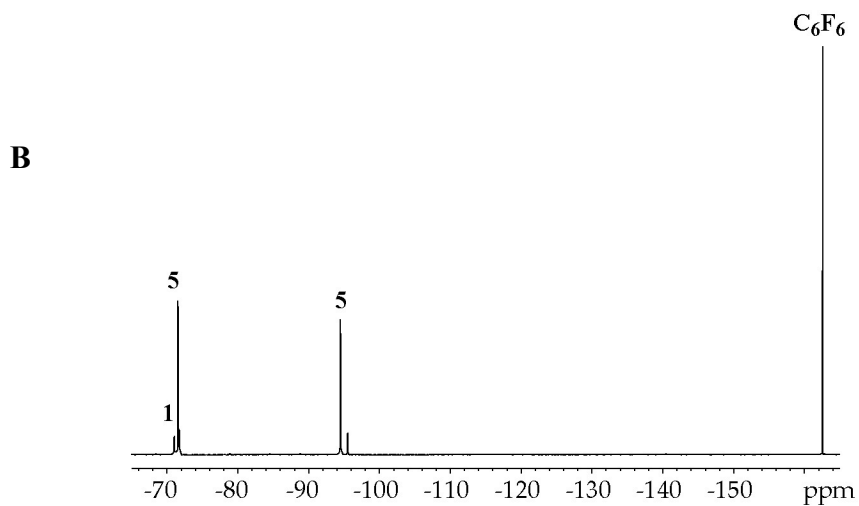
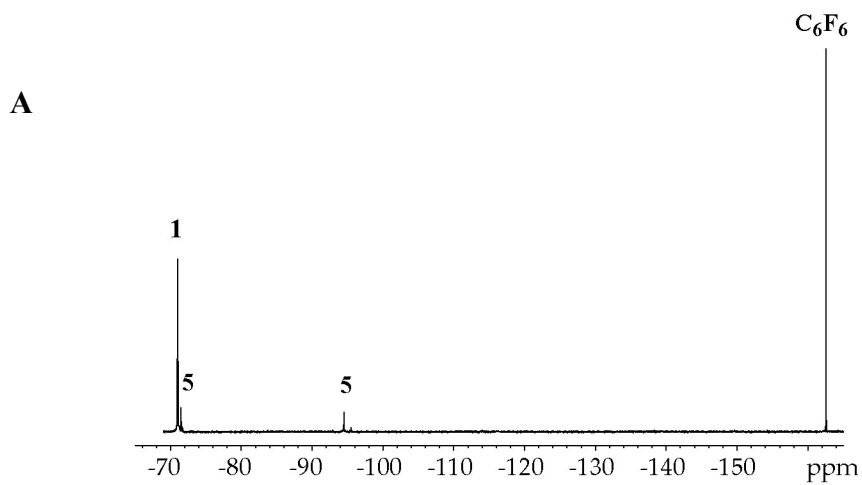
i



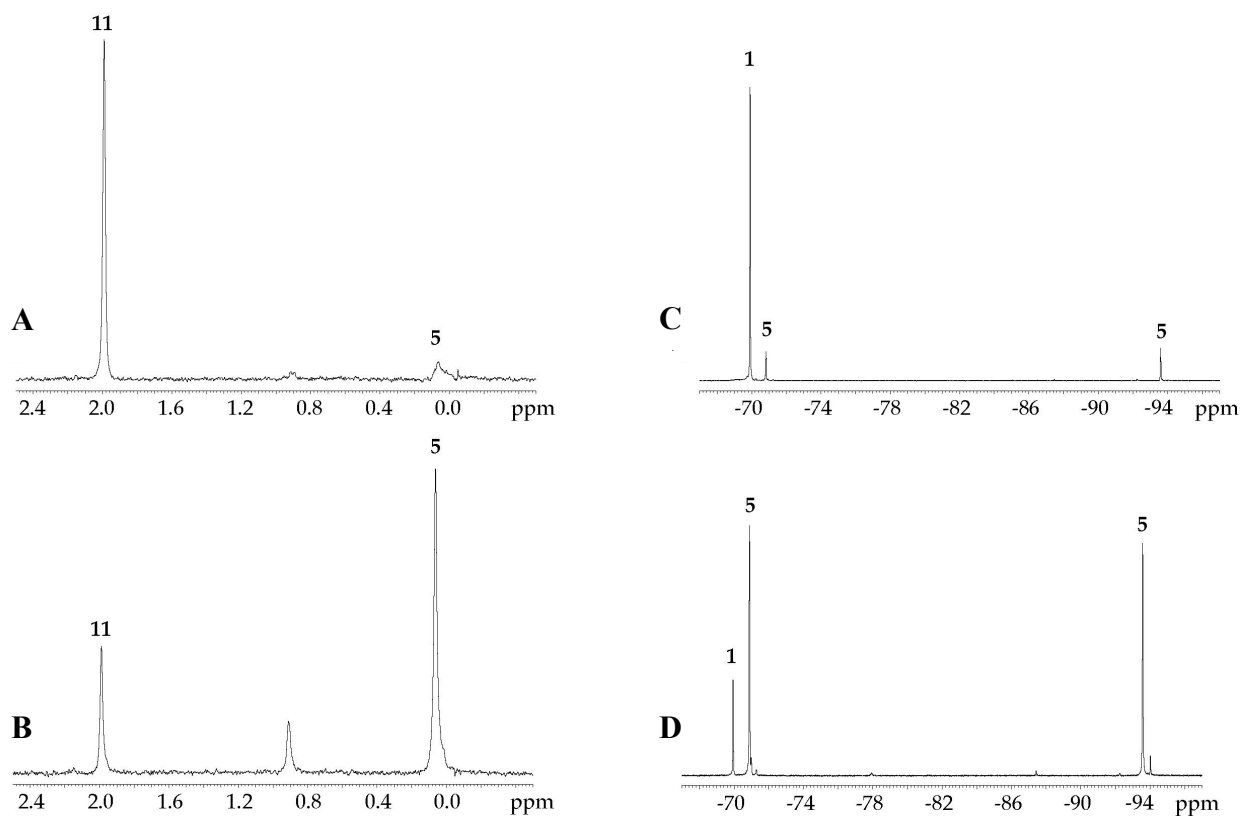
23



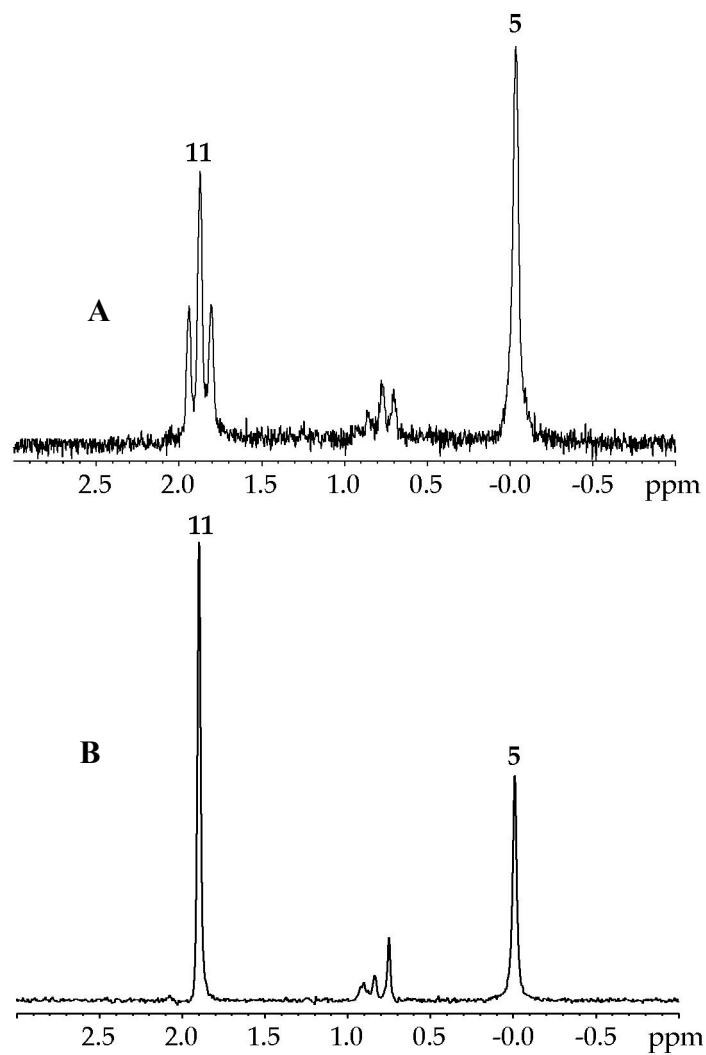
I. NMR spectra of **2** in DMSO- d_6 : (A) ^1H NMR; and (B) ^{13}C NMR.



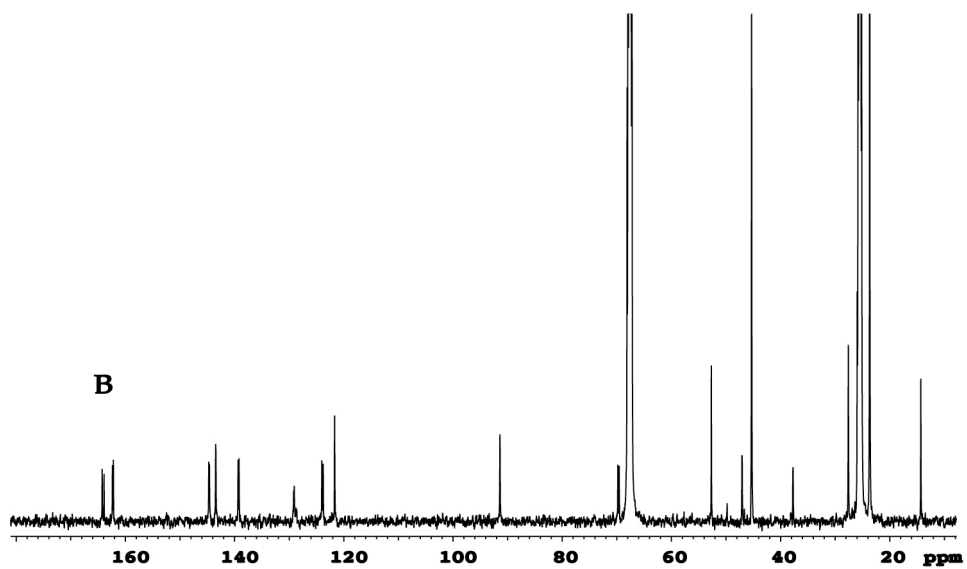
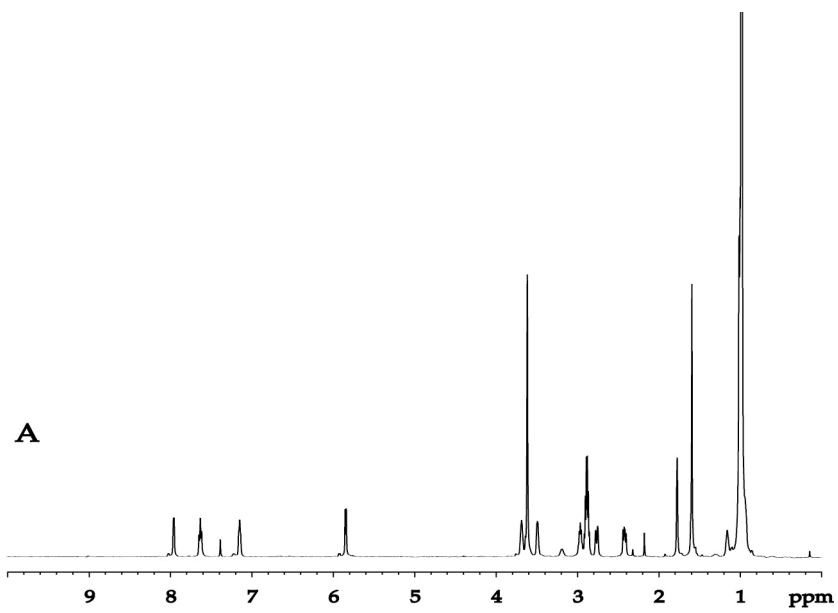
II. ^{19}F NMR spectra of 0.10 M **1** with 0.10 M LDA in neat THF at $-78\text{ }^\circ\text{C}$ showing reaction to form **5**. Hexafluorobenzene (0.60 M in neat THF) is included as an internal standard in a sealed capillary tube. Spectra were recorded (A) after 30 s aging at $-40\text{ }^\circ\text{C}$; and (B) after 10 min aging at $-40\text{ }^\circ\text{C}$.



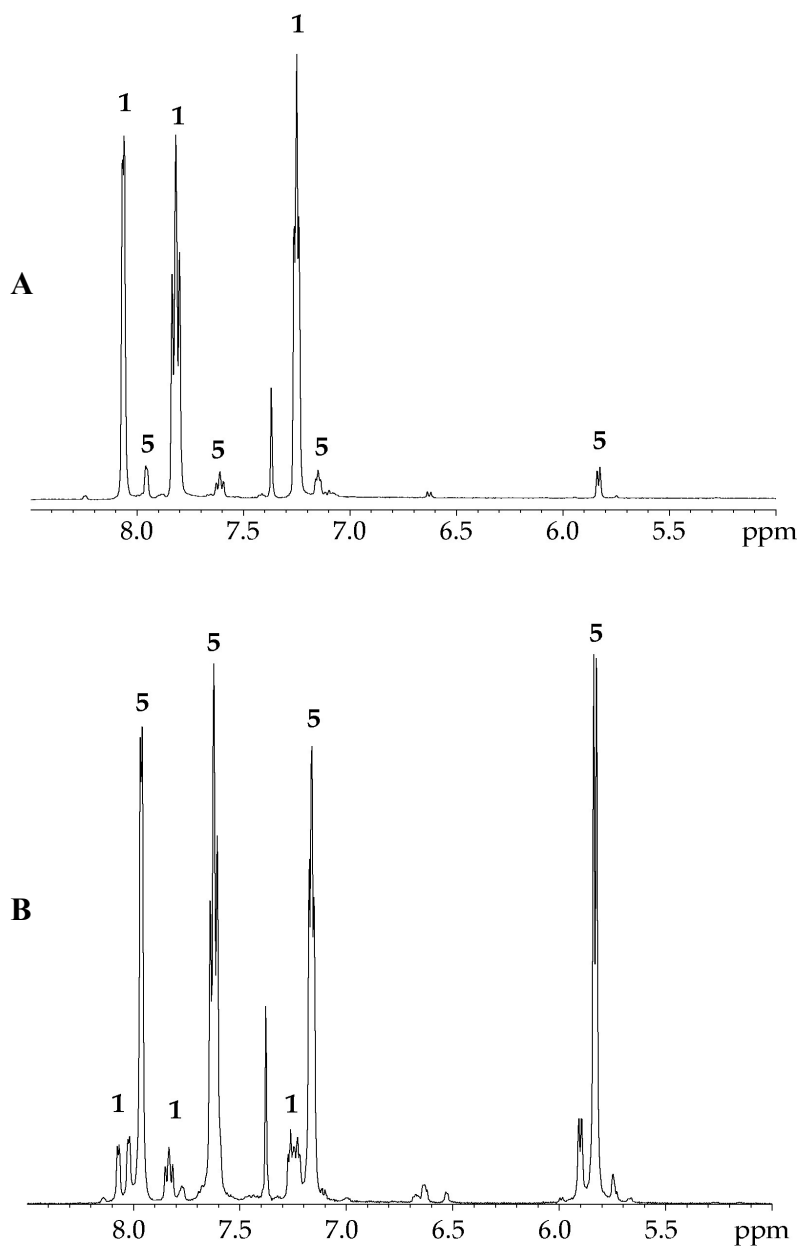
III. ^6Li and ^{19}F NMR spectra of 0.30 M **1** with 0.30 M [^6Li]LDA in neat THF at $-78\text{ }^\circ\text{C}$ showing reaction to form **5**. Spectra were recorded as follows: **(A)** ^6Li spectrum at $-40\text{ }^\circ\text{C}$ after 10 s aging; **(B)** ^6Li spectrum at $-40\text{ }^\circ\text{C}$ after 3 min aging; **(C)** ^{19}F spectrum at $-40\text{ }^\circ\text{C}$ after 10 s aging; and **(D)** ^{19}F spectrum at $-40\text{ }^\circ\text{C}$ after 3 min aging.



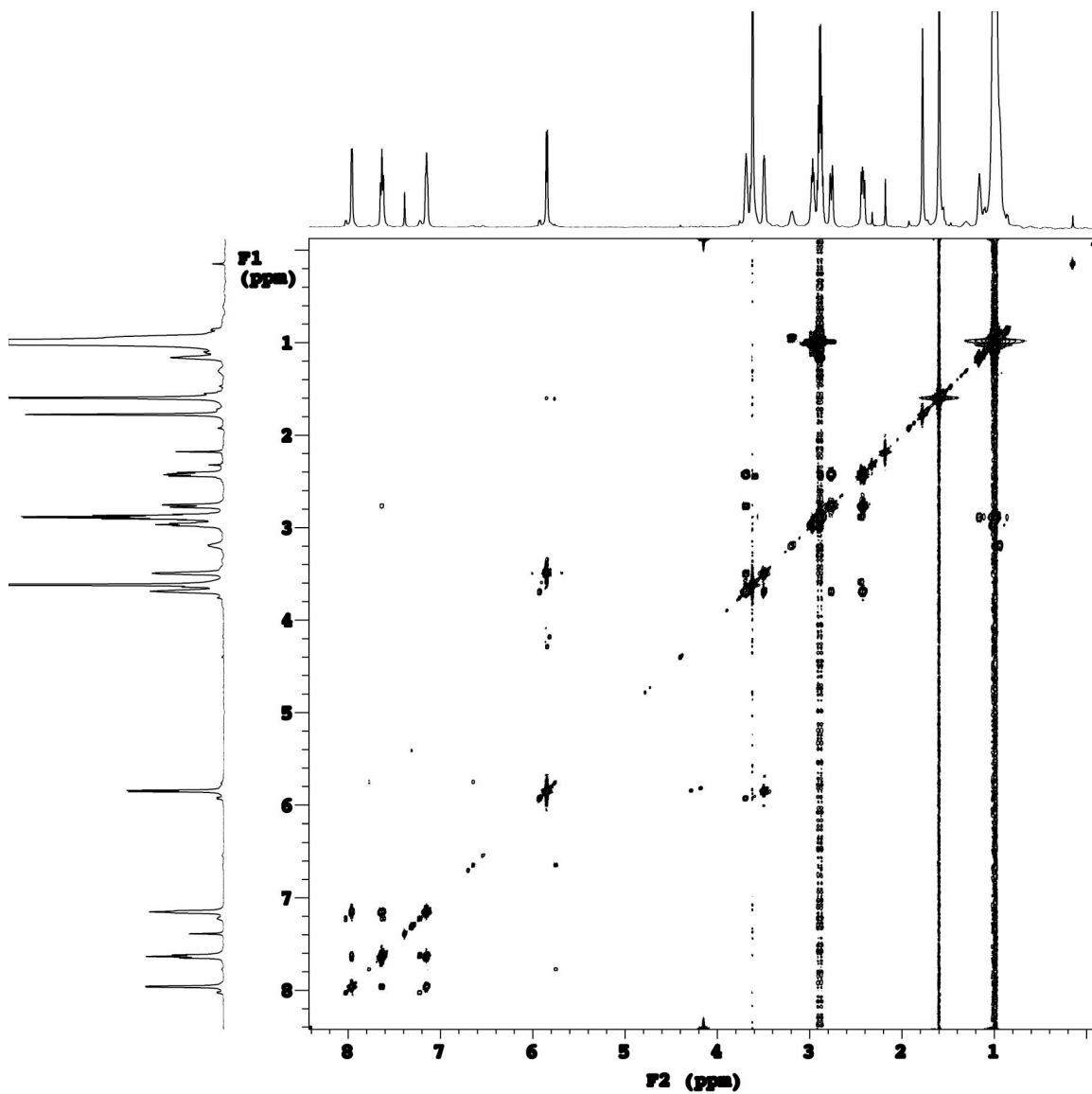
IV. ${}^6\text{Li}$ NMR spectra of 0.30 M **1** with 0.30 M [${}^6\text{Li}, {}^{15}\text{N}$]LDA in neat THF recorded at $-78\text{ }^\circ\text{C}$ after aging at $-55\text{ }^\circ\text{C}$ for 1 h showing no ${}^6\text{Li}$ - ${}^{15}\text{N}$ coupling of **5**. (A) ${}^6\text{Li}$ spectrum and (B) ${}^6\text{Li}\{{}^{15}\text{N}\}$ spectrum.



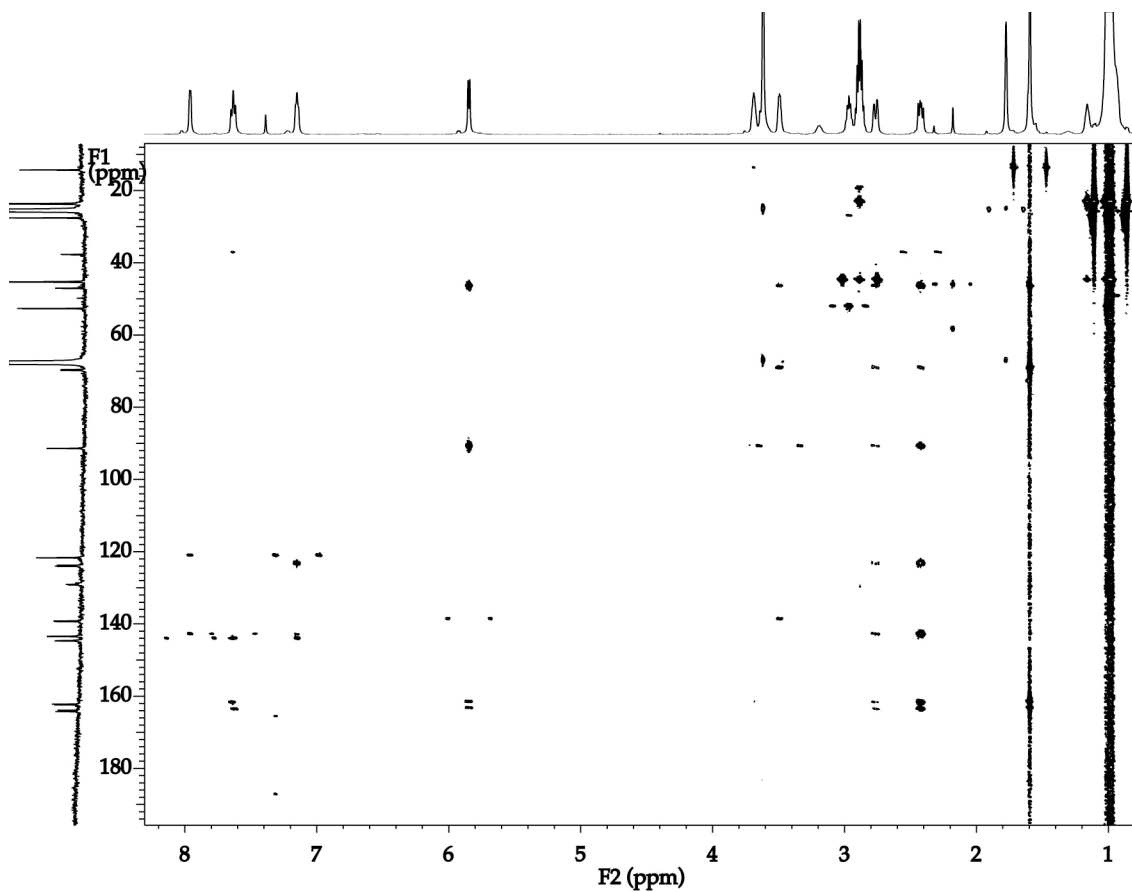
V. ^1H NMR spectra of 0.10 M **1** with 0.10 M LDA in neat THF at $-78\text{ }^\circ\text{C}$ showing reaction to form **5**. (A) ^1H NMR spectra were recorded after 30 min aging at $-40\text{ }^\circ\text{C}$; and (B) ^{13}C NMR spectra were recorded after 30 min aging at $-40\text{ }^\circ\text{C}$.



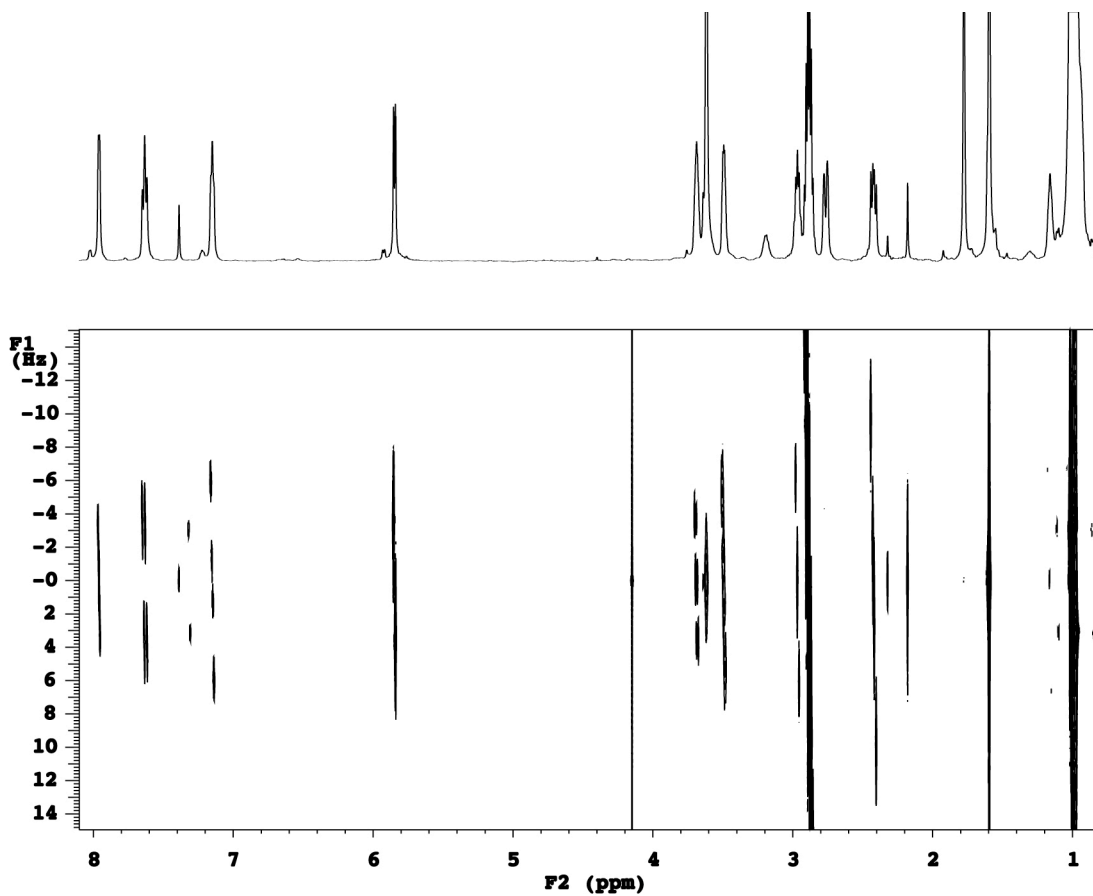
VI. ^1H NMR spectra of 0.30 M **1** with 0.30 M LDA in neat THF at $-78\text{ }^\circ\text{C}$ showing reaction to form **5**. Only aromatic and vinylic regions are included for clarity. Spectra were recorded (A) after 30 s aging at $-40\text{ }^\circ\text{C}$; and (B) after 10 min aging at $-40\text{ }^\circ\text{C}$.



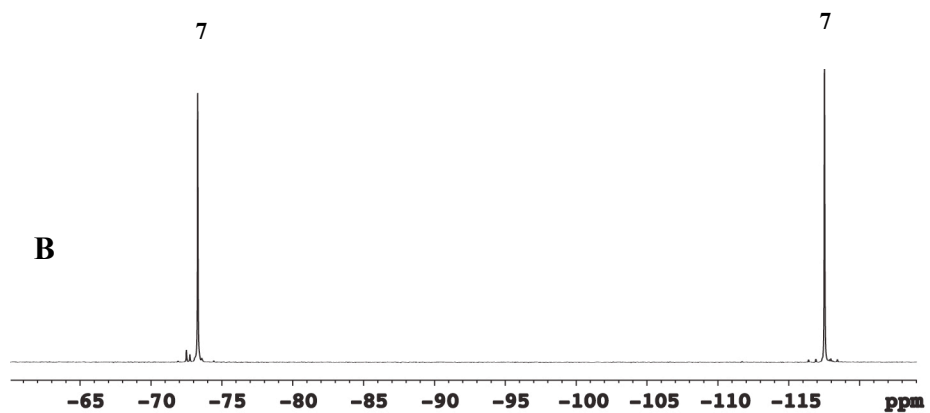
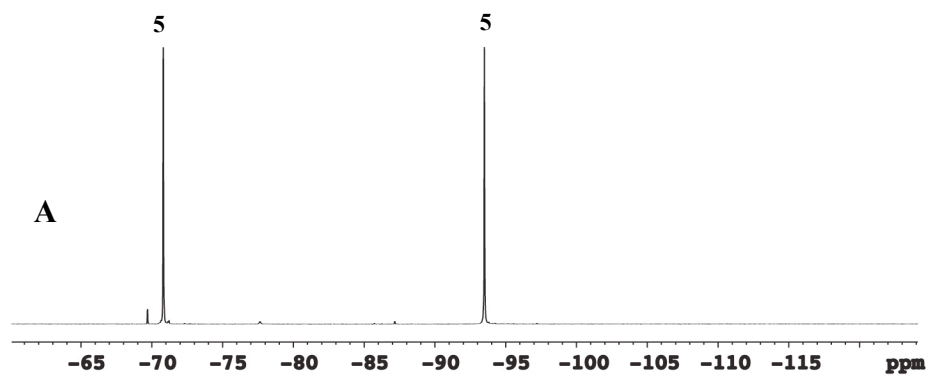
VII. $[\text{}^1\text{H}, \text{}^1\text{H}]$ COSY NMR spectrum of 0.10 M **1** with 0.10 M LDA in neat THF- d_8 at -78 $^\circ\text{C}$ showing reaction to form **5**. The spectrum was recorded after 30 min aging at -40 $^\circ\text{C}$.



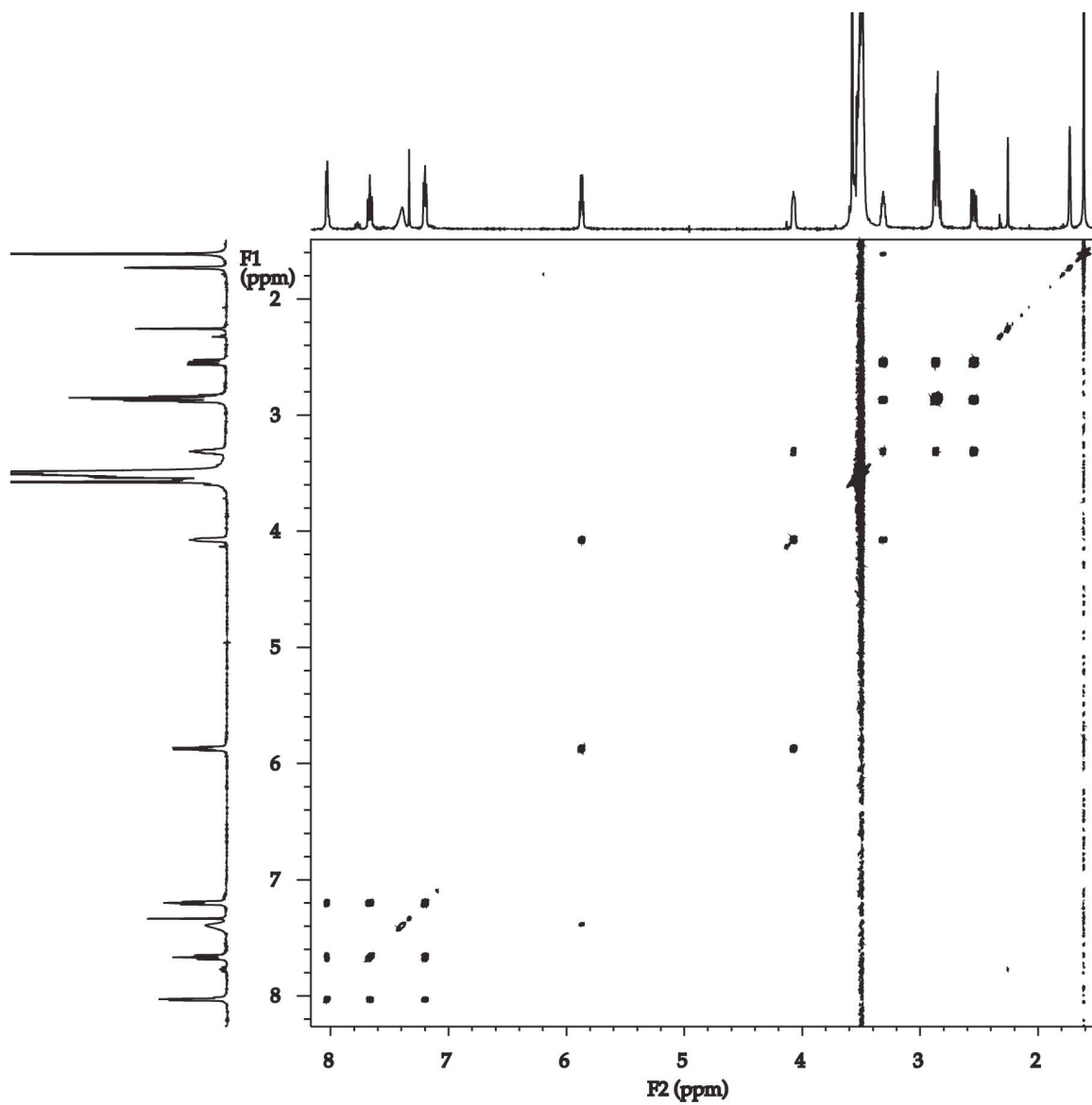
VIII. [^1H , ^{13}C]HMBC NMR spectrum of **5** revealing long range ^1H - ^{13}C heteronuclear correlation. The sample was prepared with 0.10 M **1** with 0.10 M LDA in neat THF at $-78\text{ }^\circ\text{C}$. The spectrum was recorded after 30 min aging at $-40\text{ }^\circ\text{C}$.



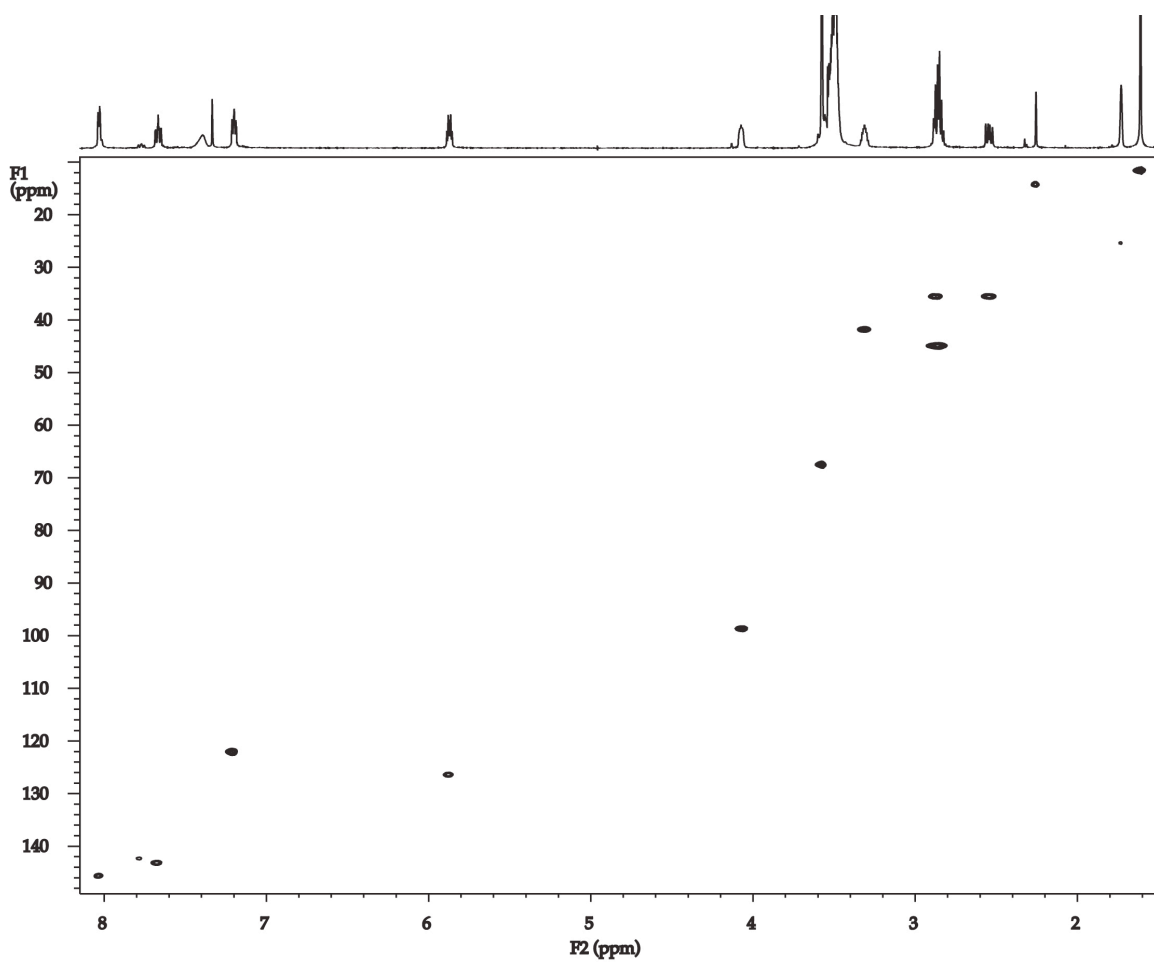
IX. $J\{^1\text{H}, ^{19}\text{F}\}$ -resolved spectrum of **5**. The sample was prepared with 0.10 M **1** with 0.10 M LDA in neat THF at $-78\text{ }^\circ\text{C}$. The spectrum was recorded after 30 min aging at $-40\text{ }^\circ\text{C}$.



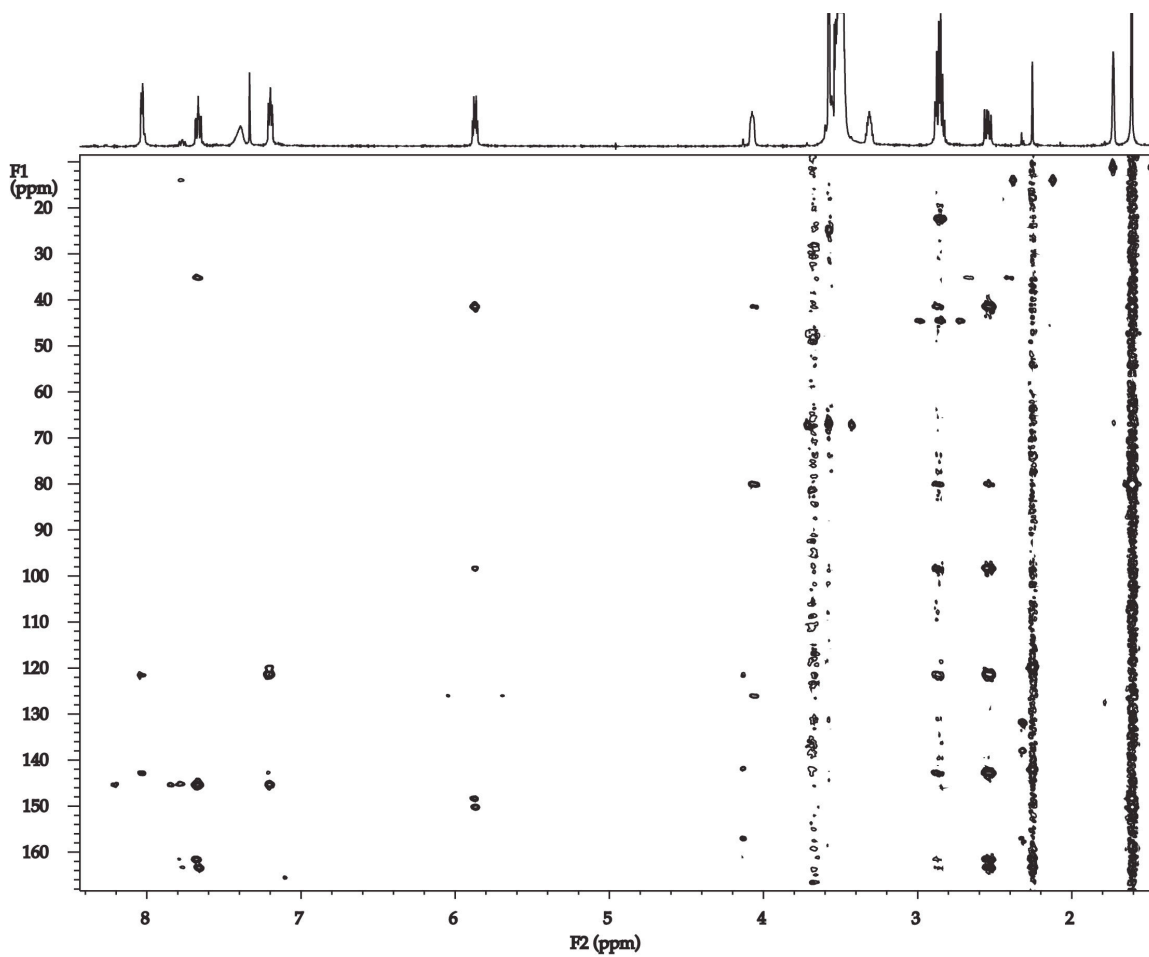
X. ^{19}F NMR spectra: (A) after complete reaction of **1** with LDA to form **5** at $-40\text{ }^\circ\text{C}$; and (B) immediately after quench of sample with $\text{H}_2\text{O}/\text{THF}$ at $-40\text{ }^\circ\text{C}$ to form dihydropyridine **7**.



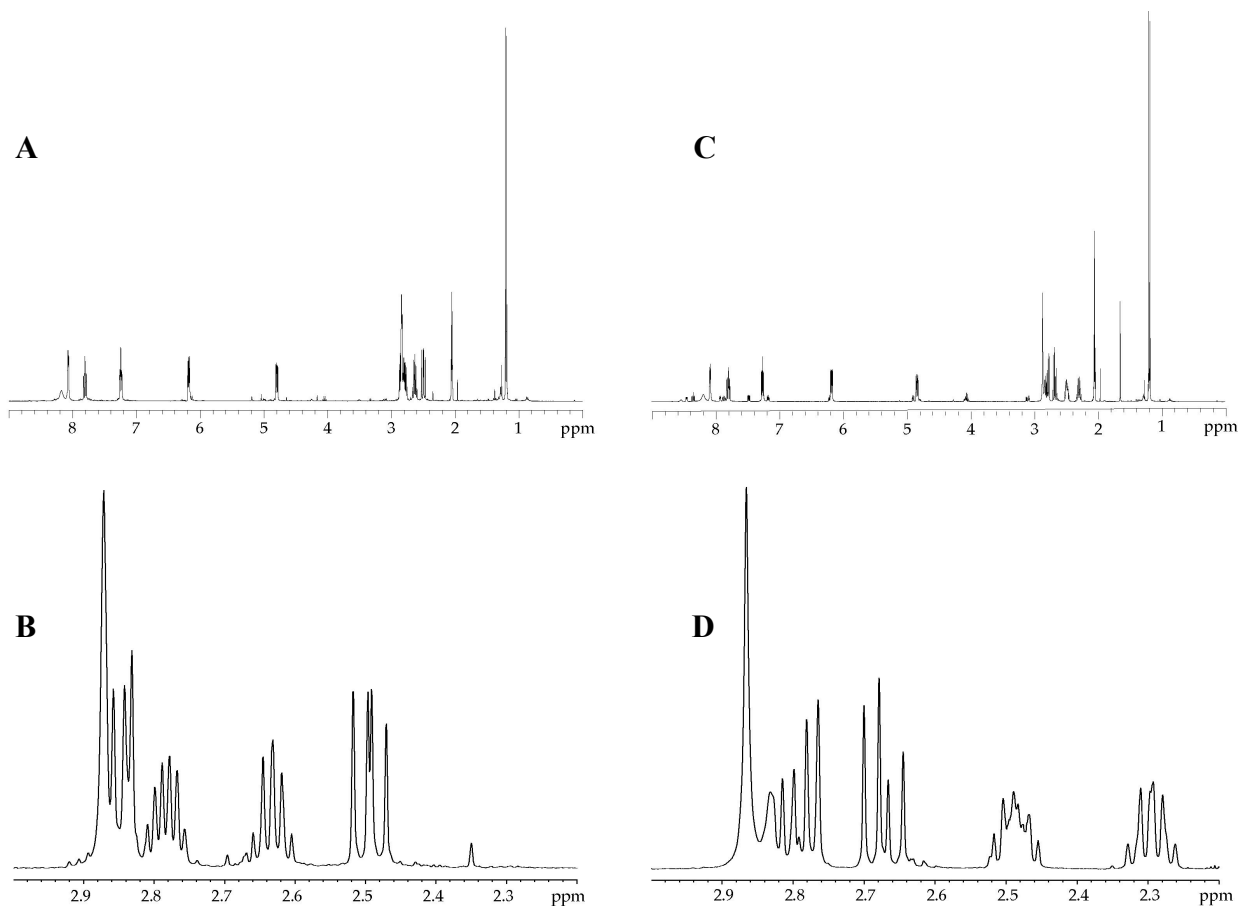
XI. [$^1\text{H}, ^1\text{H}$]COSY NMR spectrum of **7** recorded in neat $\text{THF-}d_8$ at $-70\text{ }^\circ\text{C}$.



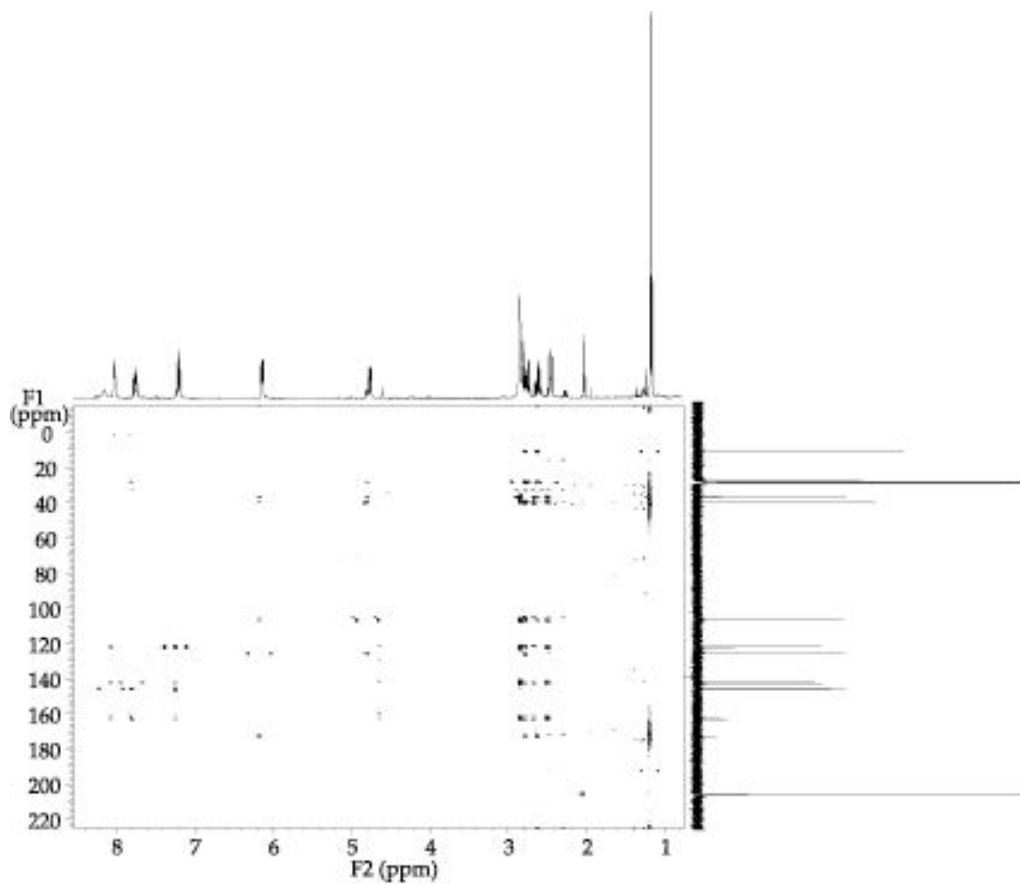
XII. [^1H , ^{13}C]HSQC NMR spectrum of **7** recorded in neat $\text{THF-}d_8$ at $-70\text{ }^\circ\text{C}$.



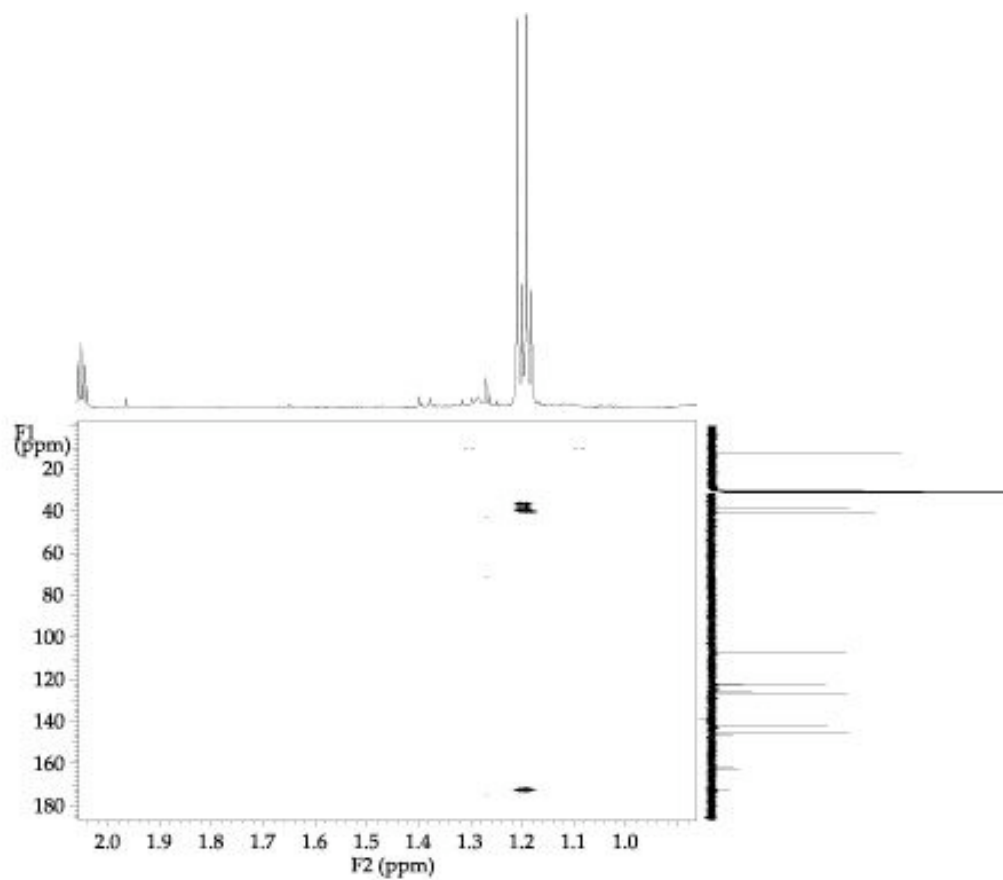
XIII. [$^1\text{H}, ^{13}\text{C}$]HMBC NMR spectrum of **7** recorded in neat $\text{THF-}d_8$ at $-70\text{ }^\circ\text{C}$.



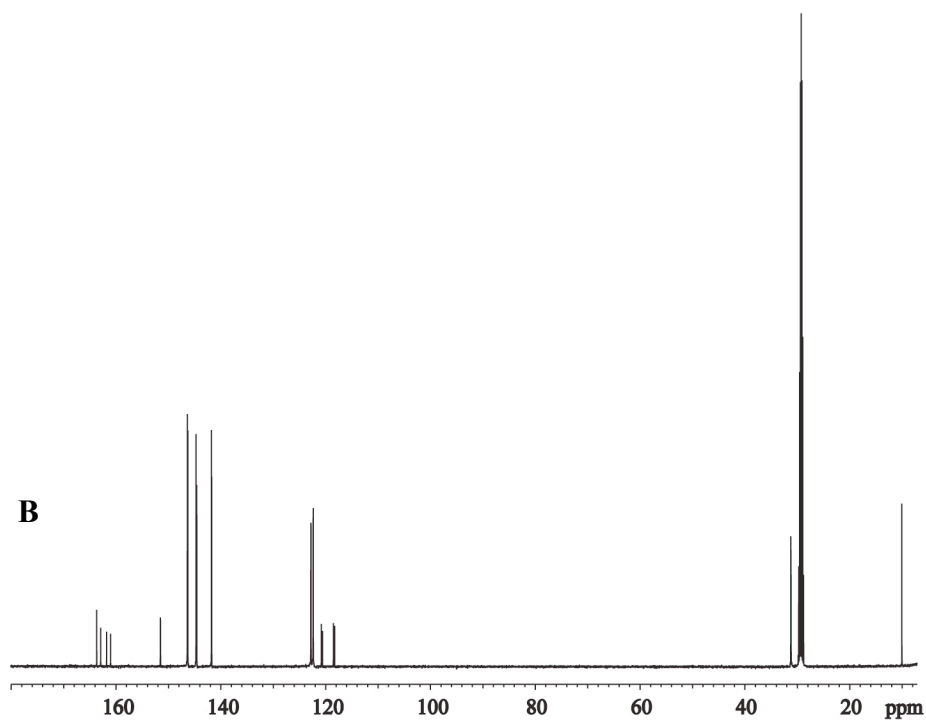
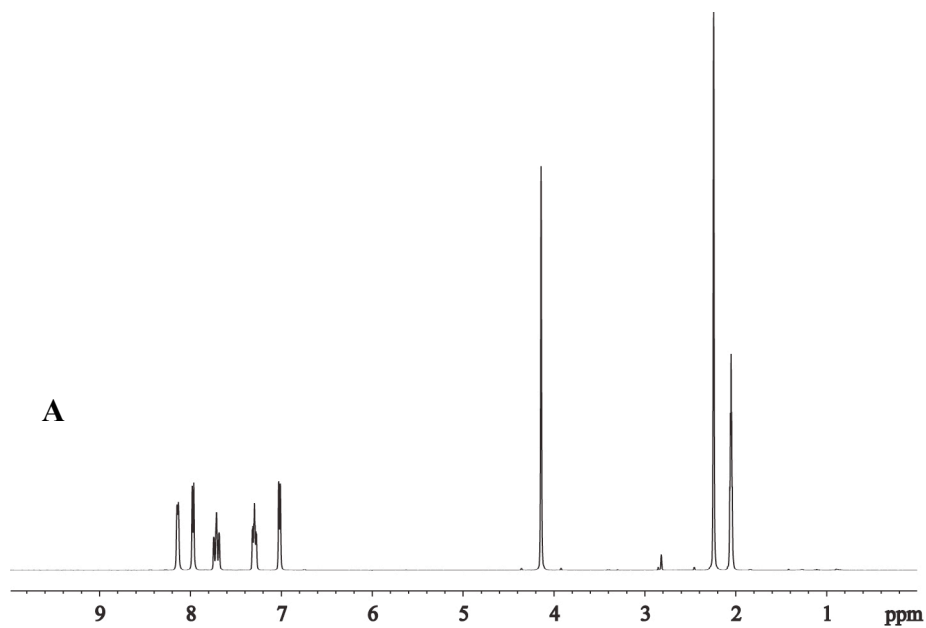
XIV. ^1H NMR spectra of major and minor diastereomers **8a** and **8b** in acetone- d_6 . **(A)** pure **8a**; **(B)** expansion of methylene region of **(A)**; **(C)** pure **8b**; and **(D)** expansion of methylene region of **(C)**.



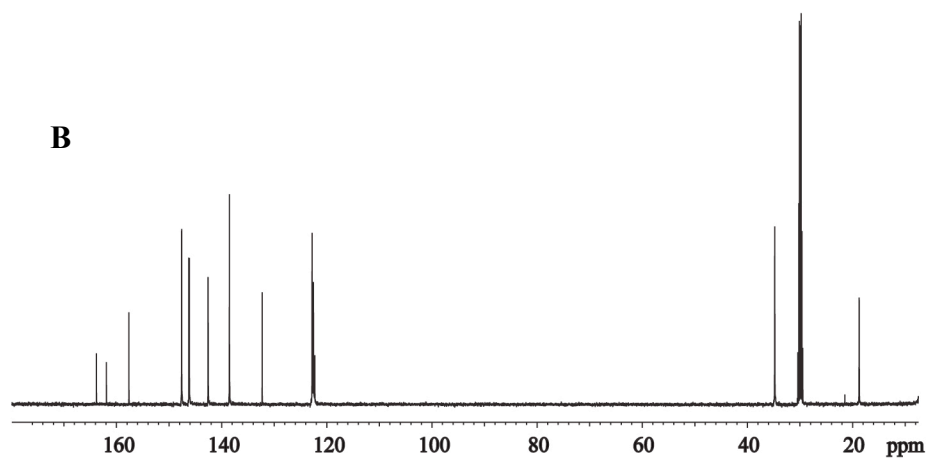
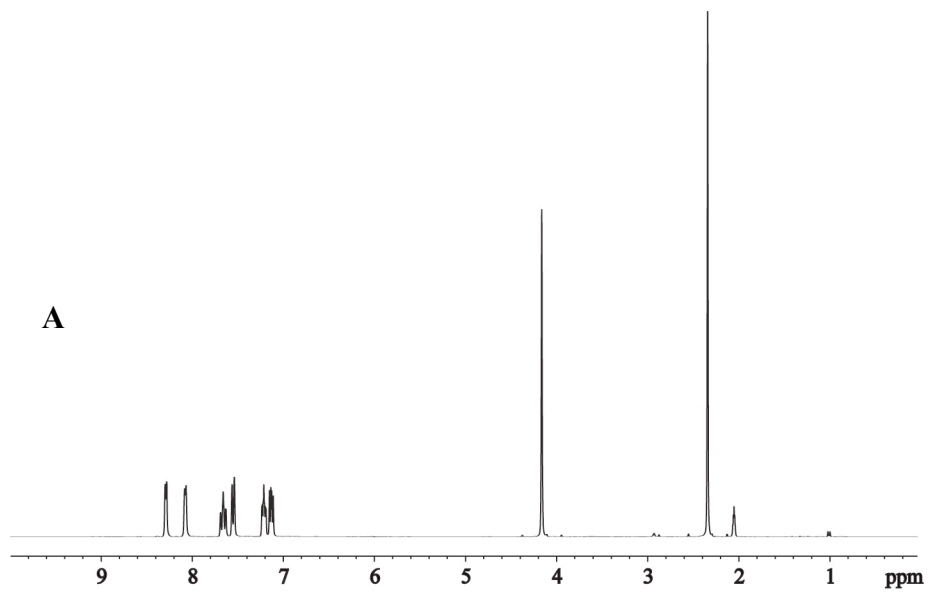
XV. [^1H , ^{13}C]HMBC NMR spectrum revealing long range ^1H - ^{13}C heteronuclear correlation in a 3:1 mixture of diastereomer **8a** and **8b** in acetone- d_6 .



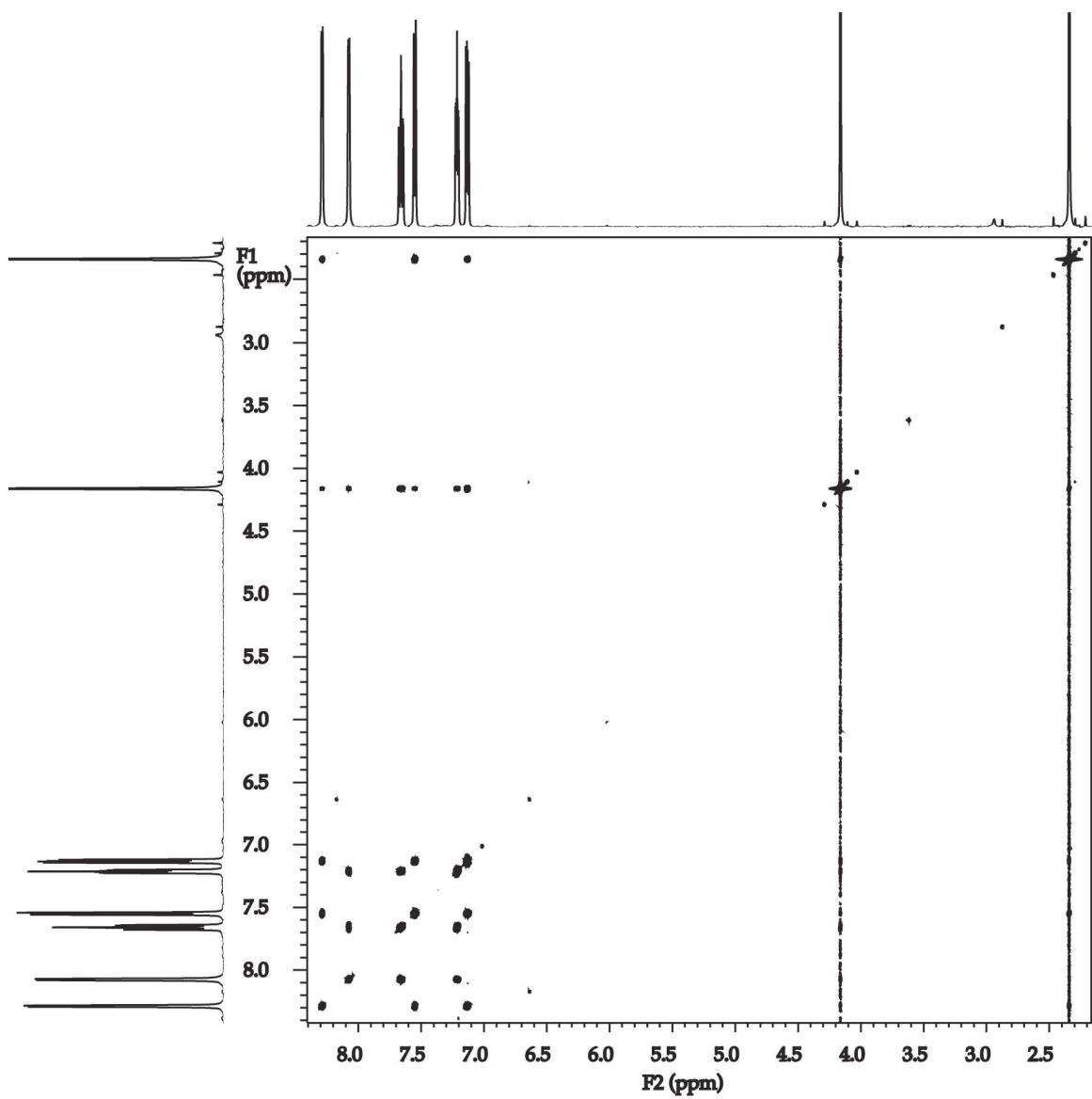
XVI. [^1H , ^{13}C]HMBC NMR spectrum revealing long range ^1H - ^{13}C heteronuclear correlation in a 3:1 mixture of diastereomer **8a** and **8b** in acetone- d_6 . ^1H dimension zoomed in on methyl region to highlight lack of ^1H methyl- ^{13}C vinyl long range correlation.



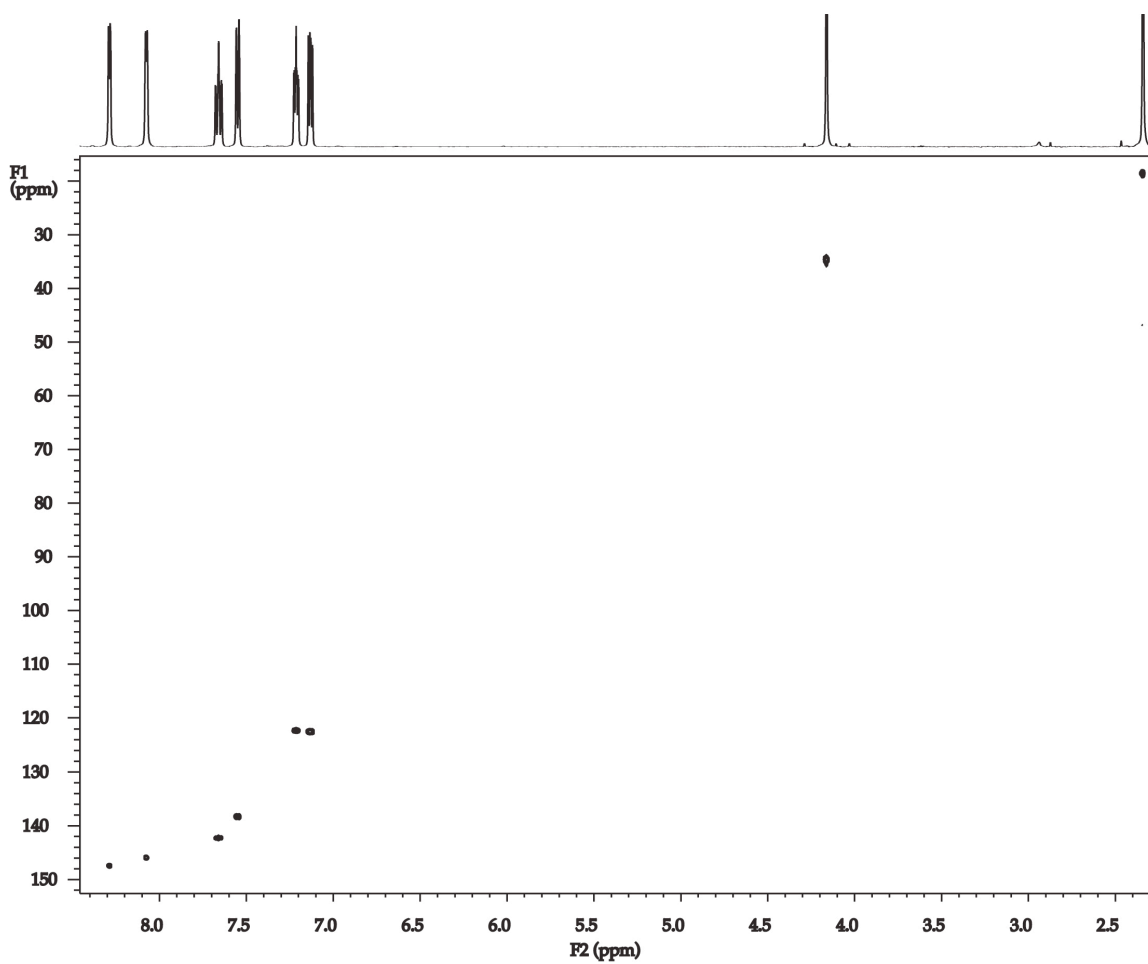
XVII. NMR spectra of aromatized 1,4-dimer **9** in acetone- d_6 : (A) ^1H spectrum; and (B) ^{13}C spectrum.



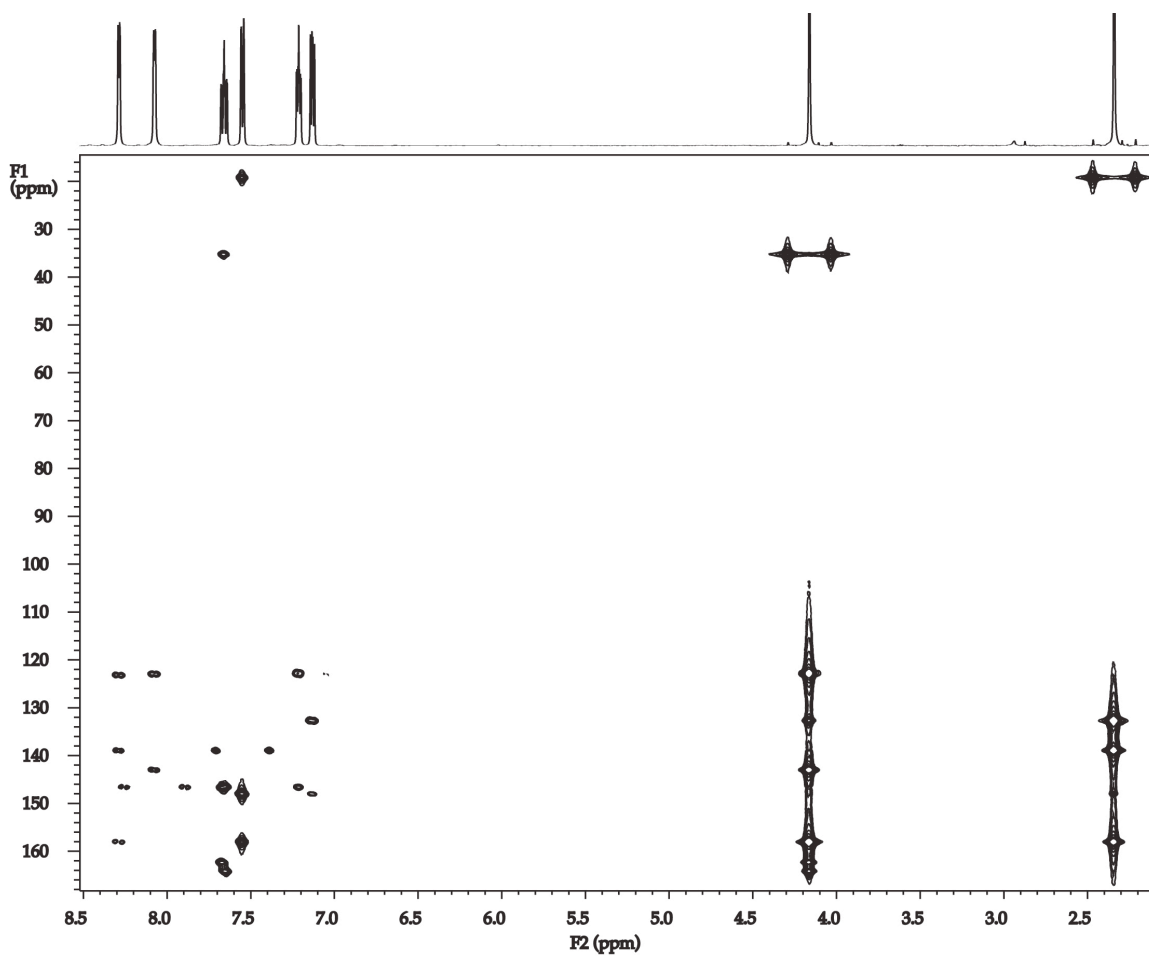
XVIII. NMR spectra of **10** in acetone- d_6 : (A) ^1H spectrum; and (B) ^{13}C spectrum.



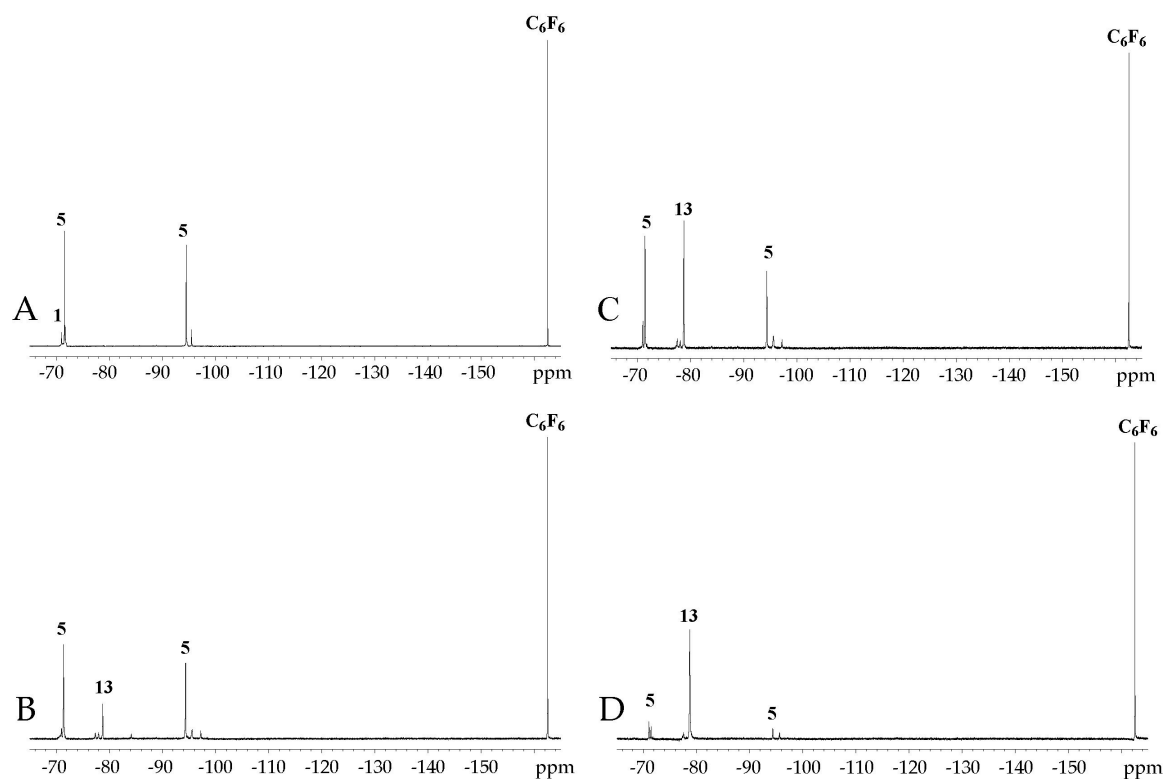
XIX. $[\text{}^1\text{H}, \text{}^1\text{H}]$ COSY NMR spectrum of **10** recorded in acetone- d_6 at 20 °C.



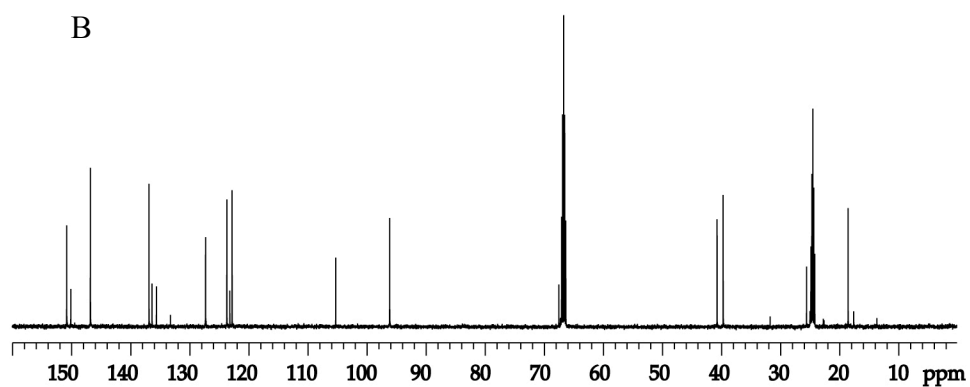
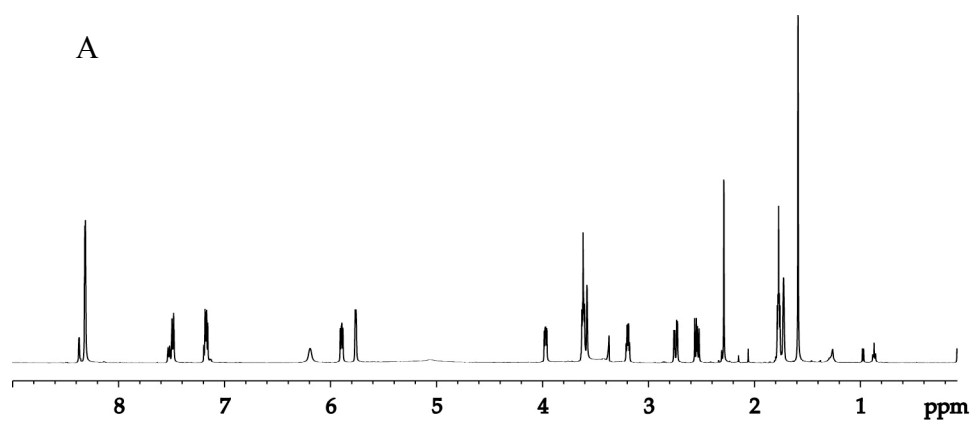
XX. $[\text{}^1\text{H}, \text{}^{13}\text{C}]$ HSQC NMR spectrum of **10** recorded in acetone- d_6 at 20 $^\circ\text{C}$.



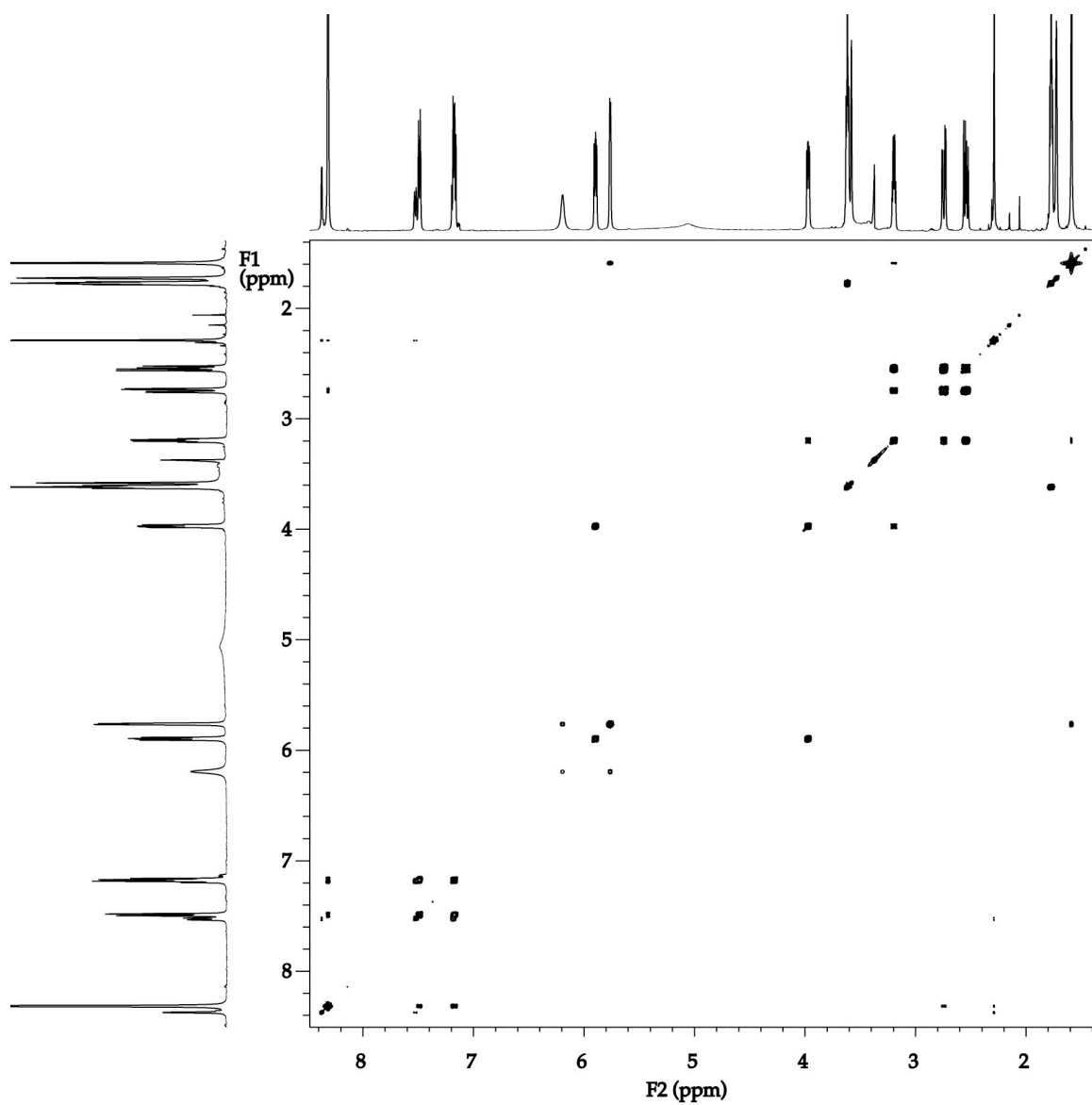
XXI. [^1H , ^{13}C]HMBC NMR spectrum of **10** recorded in acetone- d_6 at 20 °C.



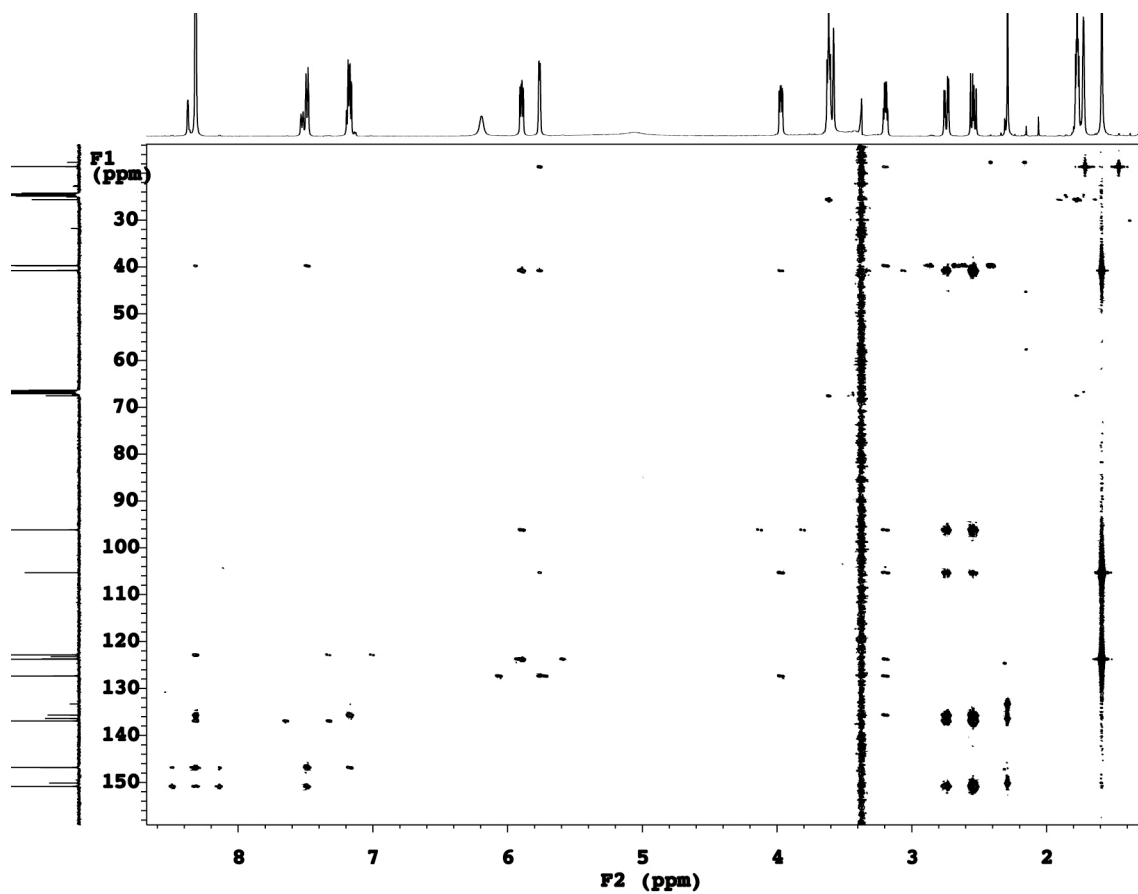
XXII. ^{19}F NMR spectra of 0.10 M **1** with 0.10 M LDA in neat THF at $-78\text{ }^\circ\text{C}$ showing reaction to form **5** and **13**. (A) Before aging; (B) after aging at $0\text{ }^\circ\text{C}$ for 1 min; (C) after aging at $0\text{ }^\circ\text{C}$ for 3 min; and (D) after aging at $0\text{ }^\circ\text{C}$ for 15 min.



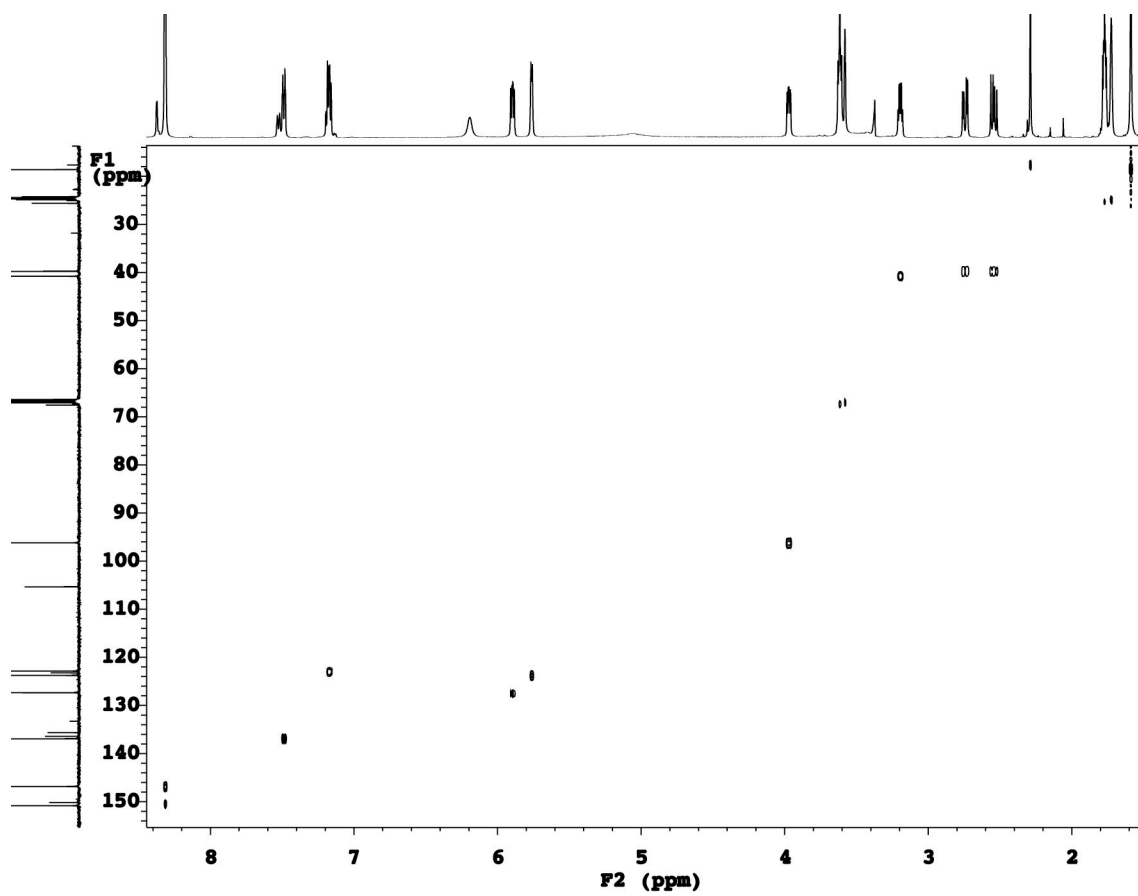
XXIII. (A) ^1H NMR spectrum of **23** was recorded in $\text{THF-}d_8$ after 30 min aging at -40°C ; and (B) ^{13}C NMR spectrum of **23** was recorded in $\text{THF-}d_8$ after 30 min aging at -40°C .



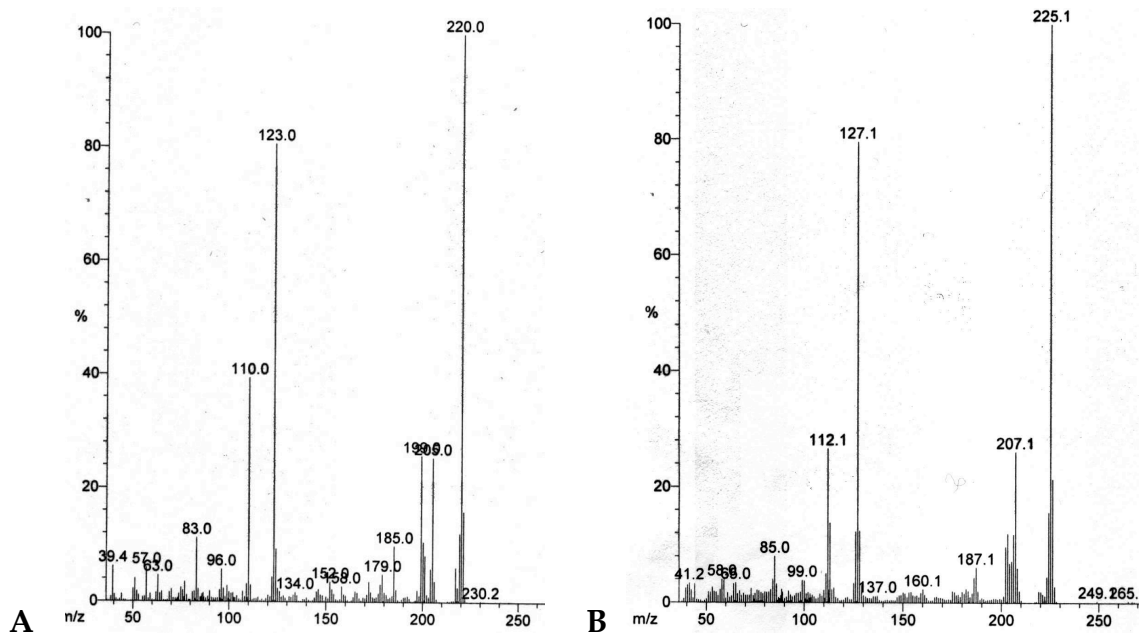
XXIV. $[\text{}^1\text{H}, \text{}^1\text{H}]$ COSY NMR spectrum of **23** recorded in neat THF- d_8 at 20 °C.



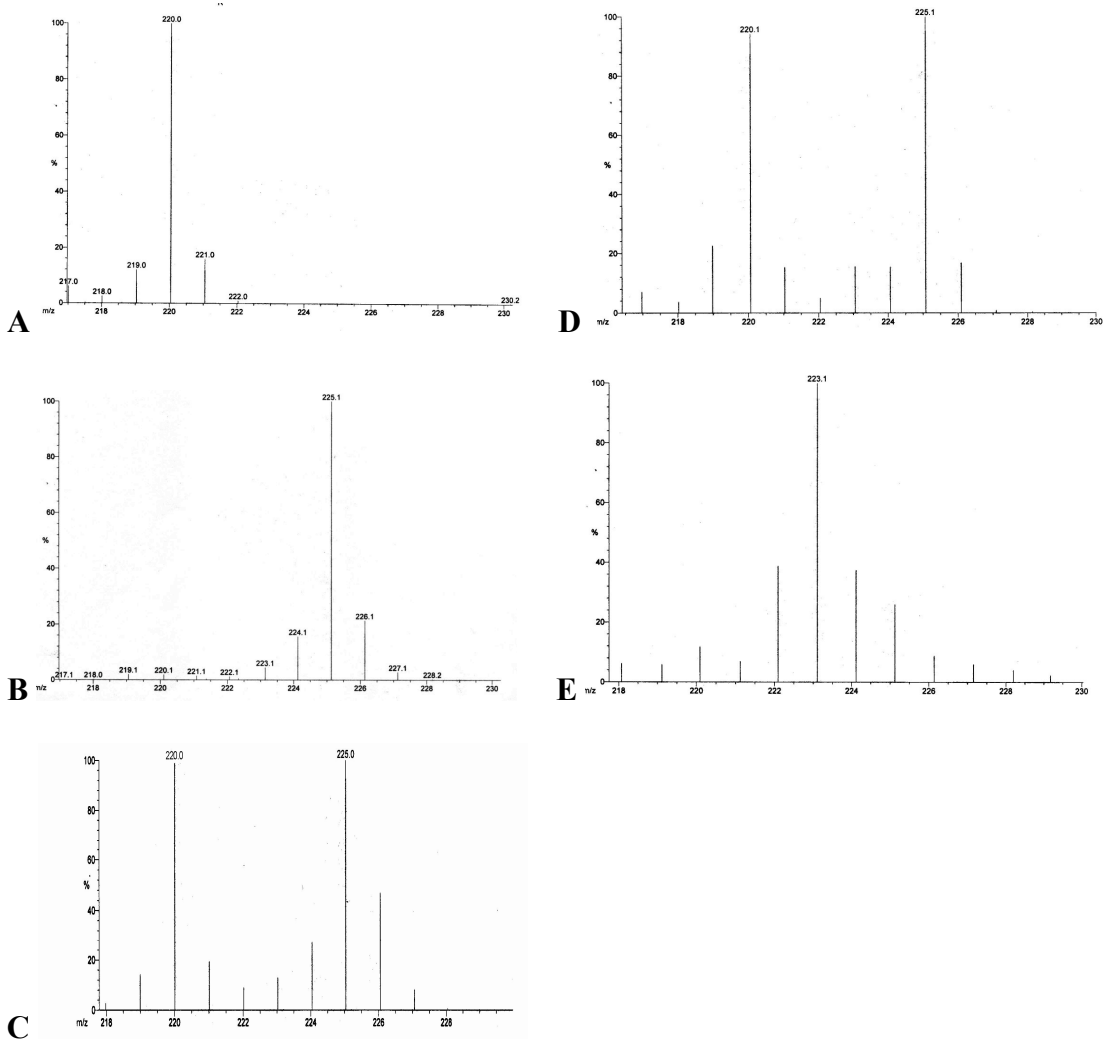
XXV. [^1H , ^{13}C]HMBC NMR spectrum of **23** recorded in neat $\text{THF-}d_8$ at 20 °C.



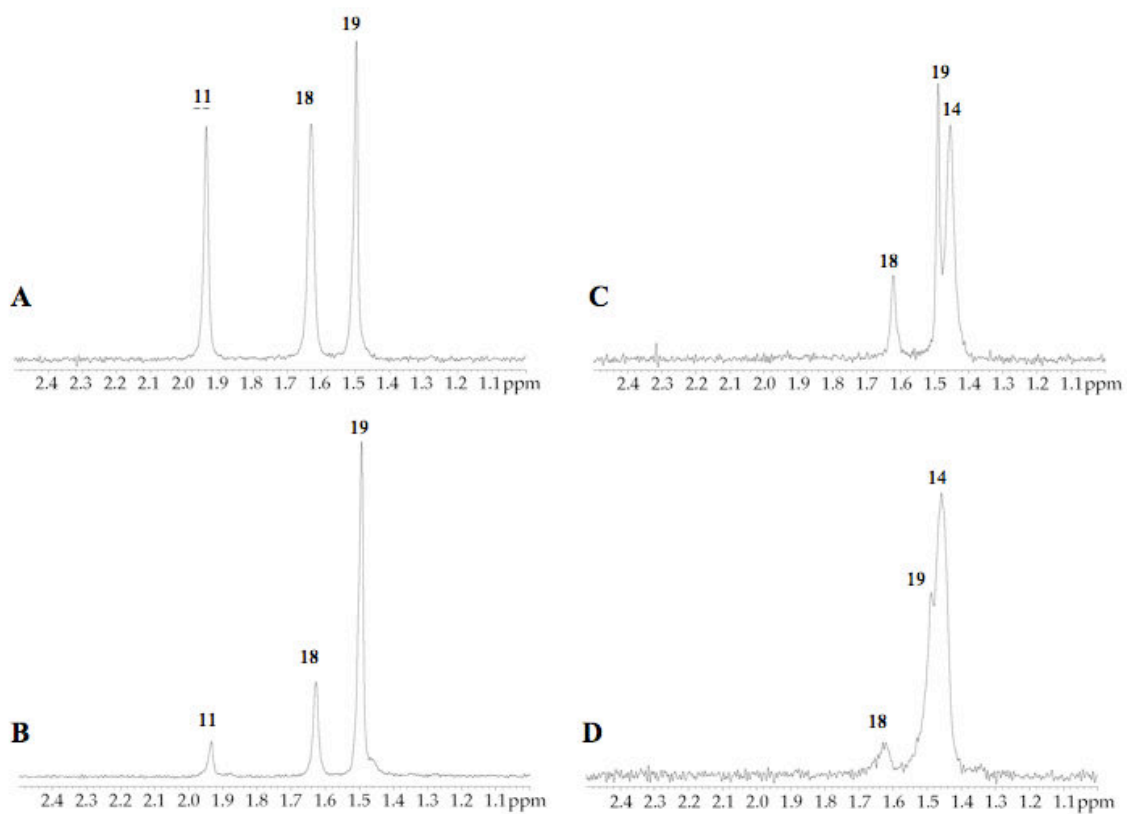
XXVI. [^1H , ^{13}C]HSQC NMR spectrum of **23** recorded in neat $\text{THF-}d_8$ at 20 $^\circ\text{C}$



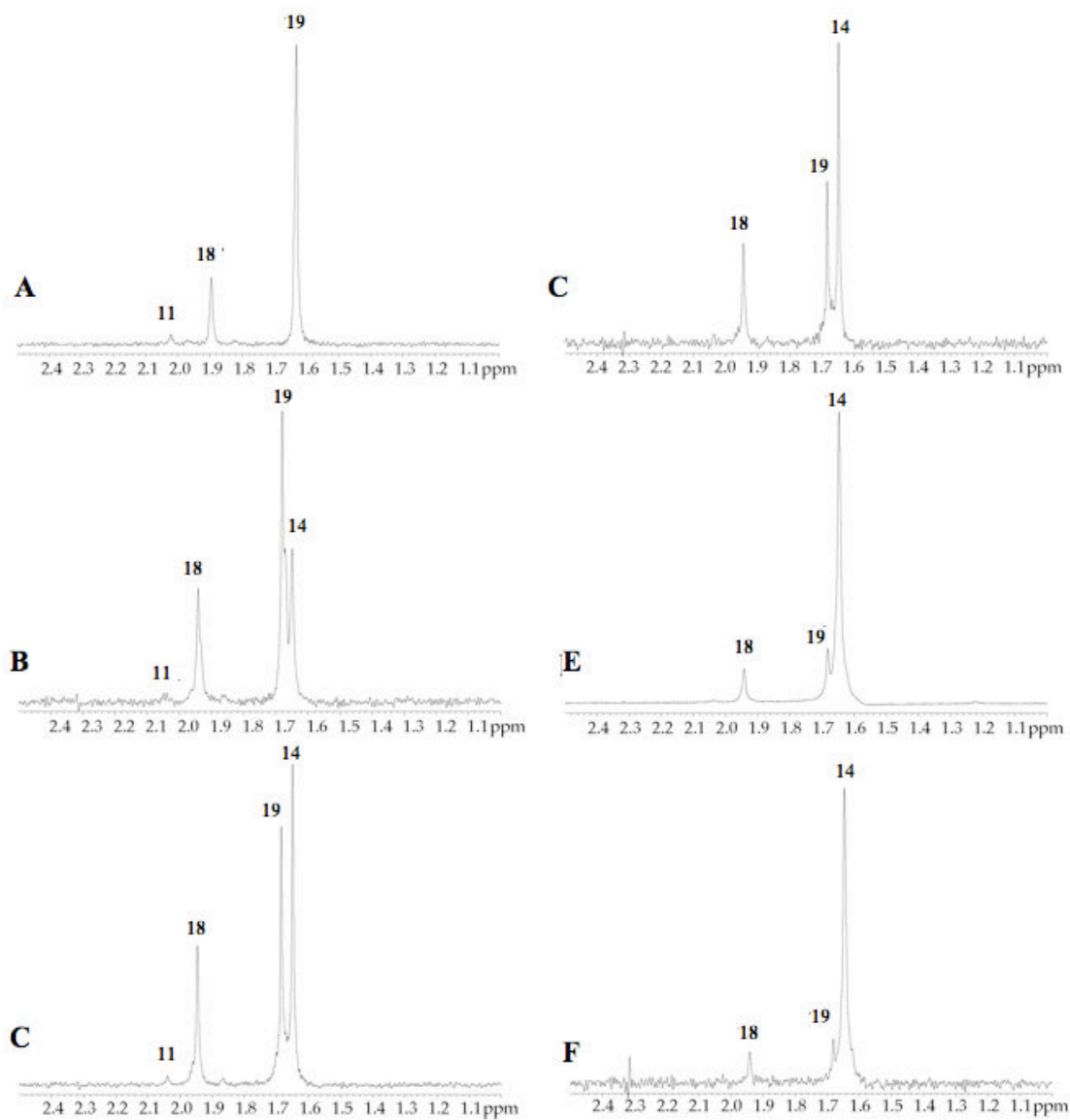
XXVII. Mass spectra of (A) **9**; and (B) **9-d₅**.



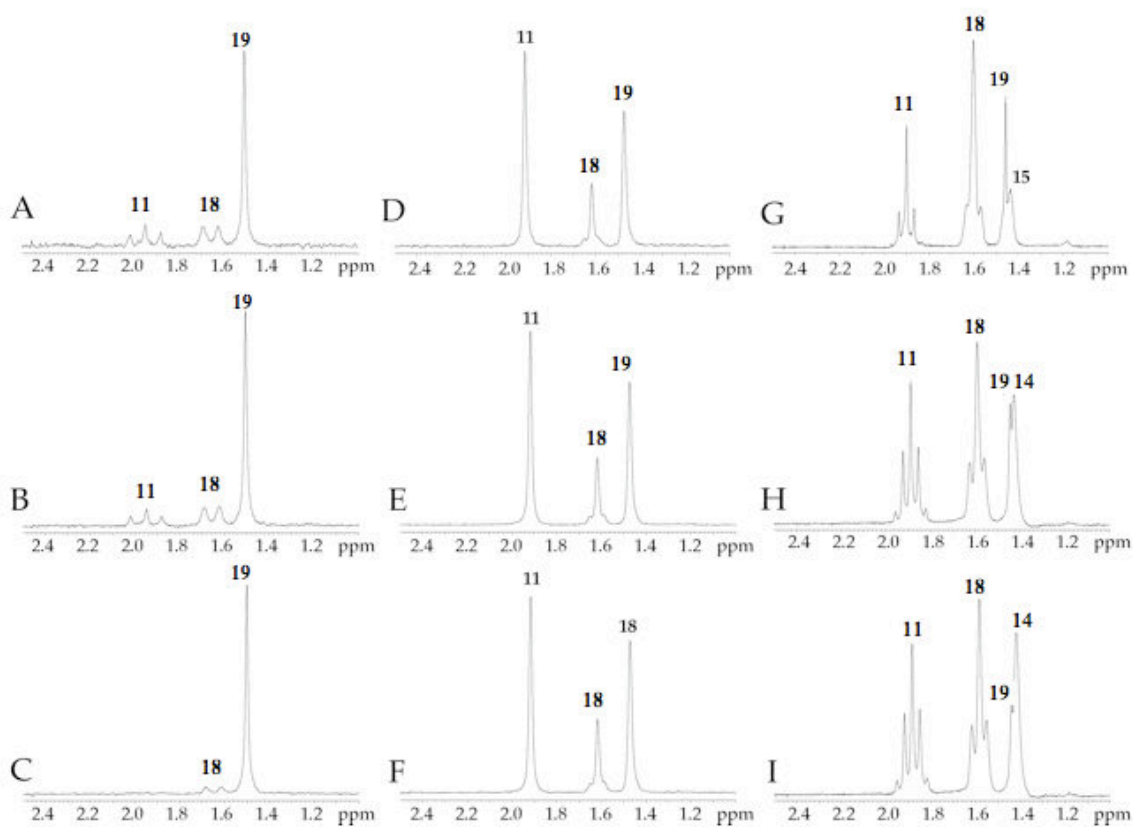
XXVIII. Expansion of M^+ peak region of mass spectra. (A) $9-d_0$; (B) $9-d_5$; (C) $9-d_0$ and $9-d_5$ resulting from quench of independently prepared solutions of $5-d_0$ and $5-d_5$ mixed together and aged at $-78\text{ }^\circ\text{C}$ for 7 min; (D) $9-d_0$ and $9-d_5$ resulting from quench of independently prepared solutions of $5-d_0$ and $5-d_5$ mixed together and aged at $-78\text{ }^\circ\text{C}$ for 1.5 min; and (E) $9-d_0$ and $9-d_5$ resulting from quench of independently prepared solutions of $5-d_0$ and $5-d_5$ mixed together and aged at $-40\text{ }^\circ\text{C}$ for 60 min.



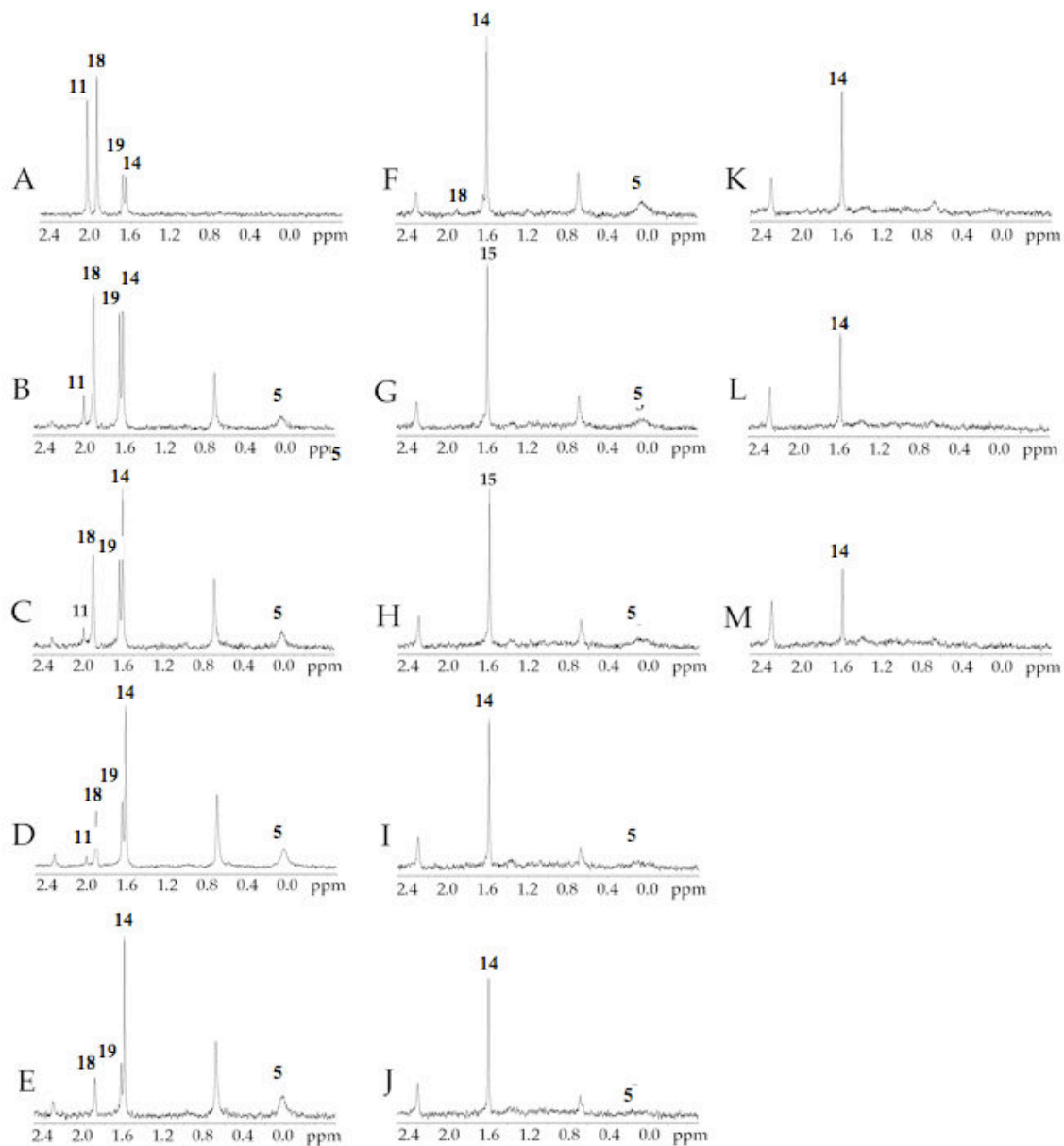
XXIX. ^6Li NMR spectra of 0.20 M **6** in neat THF. (A) Recorded at $-90\text{ }^\circ\text{C}$ after addition of 0.20 M PhCN to 0.20 M ^6Li LDA and 2 hours aging at $-90\text{ }^\circ\text{C}$; (B) recorded at $-90\text{ }^\circ\text{C}$ after 1 hr aging at $-60\text{ }^\circ\text{C}$; (C) recorded at $-90\text{ }^\circ\text{C}$ after 4 min aging at $-40\text{ }^\circ\text{C}$; and (D) recorded at $-90\text{ }^\circ\text{C}$ after 4 hours aging at $-40\text{ }^\circ\text{C}$.



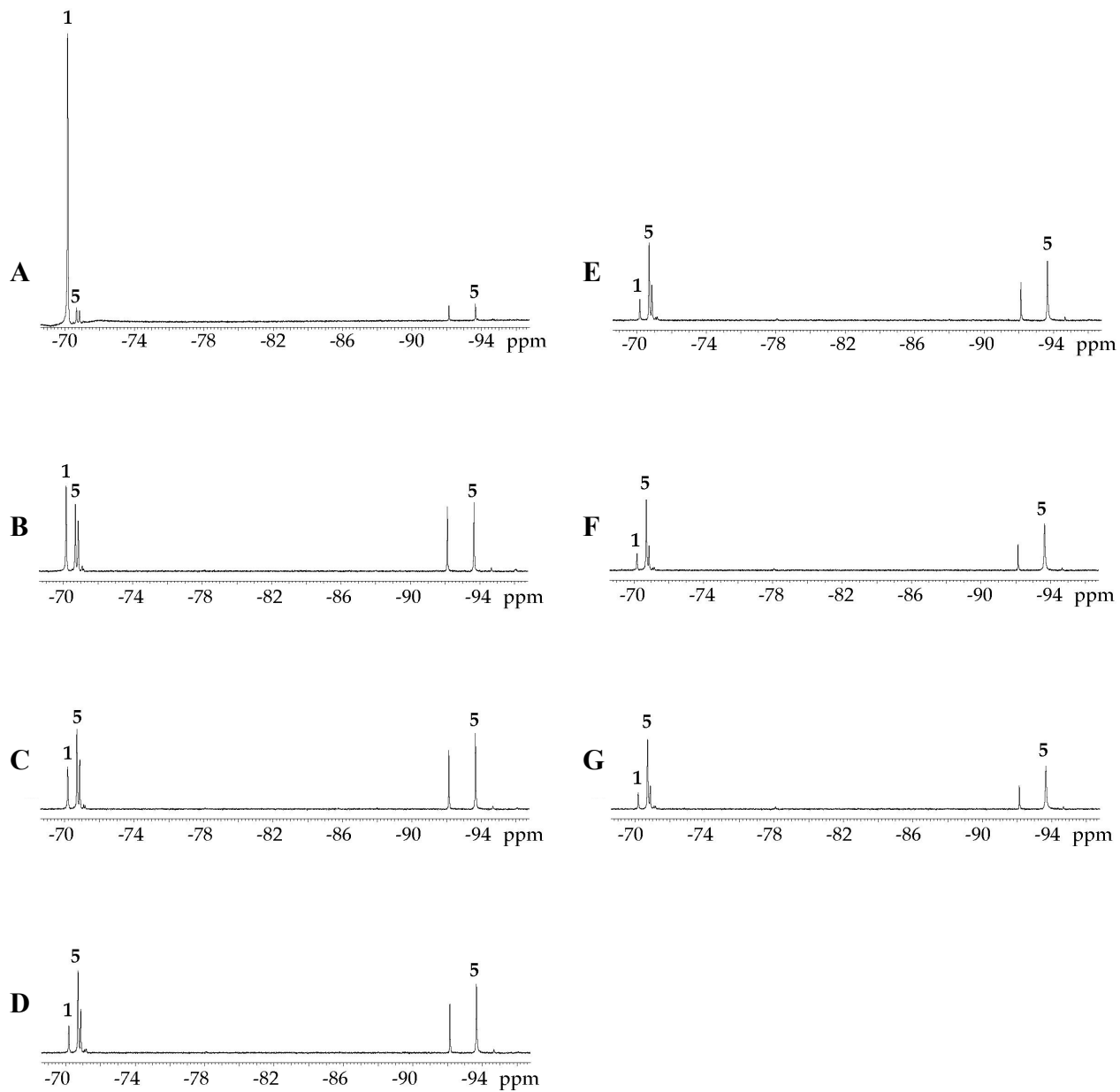
XXX. ^6Li NMR spectra of 0.20 M **6** in neat THF. (A) Recorded at $-50\text{ }^\circ\text{C}$; (B) recorded at $-40\text{ }^\circ\text{C}$ after 4 min aging at $-40\text{ }^\circ\text{C}$; (C) recorded at $-40\text{ }^\circ\text{C}$ after 8 min aging at $-40\text{ }^\circ\text{C}$; (D) recorded at $-40\text{ }^\circ\text{C}$ after 12 min aging at $-40\text{ }^\circ\text{C}$; (E) recorded at $-40\text{ }^\circ\text{C}$ after 25 min aging at $-40\text{ }^\circ\text{C}$; and (F) recorded at $-40\text{ }^\circ\text{C}$ after 30 min aging at $-40\text{ }^\circ\text{C}$.



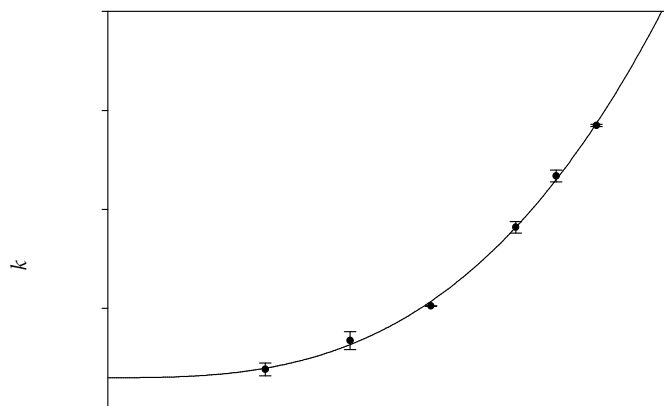
XXXI. ^6Li NMR spectra of 0.20 M [^6Li , ^{15}N]LDA plus 0.26 M PhCN in neat THF at -90 $^\circ\text{C}$. After (A) 5 min at -78 $^\circ\text{C}$ and 9 min at -90 $^\circ\text{C}$; (B) 3 additional min at -90 $^\circ\text{C}$; (C) 27 additional min at -90 $^\circ\text{C}$; (D) 4 min after addition of 0.20 M [^6Li]LDA; (E) 13 min after addition; (F) 18 min after addition; (G) warming to -40 $^\circ\text{C}$ for 9 min; (H) warming to -40 $^\circ\text{C}$ for 49 min; and (I) warming to -40 $^\circ\text{C}$ for 110 min.



XXXII. ${}^6\text{Li}$ spectra of 0.10 M **6** and 0.10 M [${}^6\text{Li}$]LDA in neat THF recorded at $-40\text{ }^\circ\text{C}$ showing reaction with 1.0 eq **1**. (A) Before addition of **1**; after (B) 8 min reaction; (C) 16 min reaction; (D) 35 min reaction; (E) 45 min reaction; (F) after 73 min reaction; (G) 101 min reaction; (H) 129 min reaction; (I) 157 min reaction; (J) 185 min reaction; (K) 241 min reaction; (L) 353 min reaction; and (M) 465 min reaction.

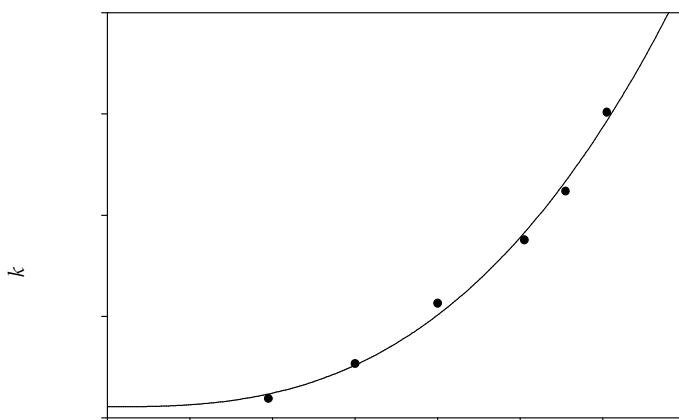


XXXIII. ^{19}F NMR spectra of 0.10 M **6** with 0.10 M LDA in neat THF at $-40\text{ }^\circ\text{C}$ showing reaction with 1.0 equiv of **1**. After (A) 20 seconds reaction; (B) 16 min reaction; (C) 32 min reaction; (D) 49.1 min reaction; (E) 65 min reaction; (F) 98 min reaction; and (G) 108 min reaction.



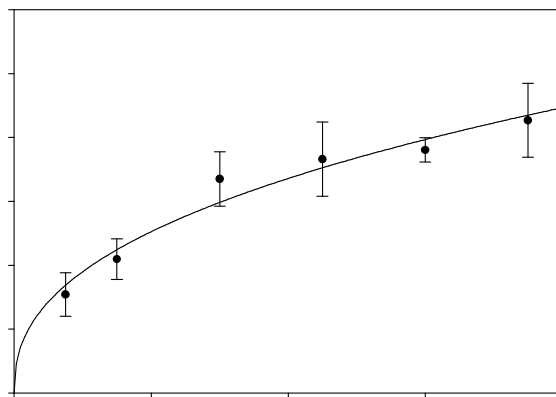
XXXIV. Plot of k_{obsd} vs [THF] in pentane for the deprotonation of 2-fluoro-3-methylpyridine (**1**, 0.01 M) by LDA (0.20 M) as determined by following loss of **1** at -20 °C by ^{19}F NMR. The curve depicts an unweighted least-squares fit to $k_{\text{obsd}} = a + k[\text{THF}]^n$ ($a = 1.50 \pm 0.28$, $k = (9.08 \pm 4.36) \times 10^{-3}$, $n = 2.91 \pm 0.19$).

[THF] (M)	$k_{\text{obsd}1}$ (s^{-1})	$k_{\text{obsd}2}$ (s^{-1})	$k_{\text{obsd}avg}$ (s^{-1})
3.9	$0.00169 \pm 3\text{E-}5$	$0.00215 \pm 2\text{E-}5$	$0.00192 \pm 3\text{E-}4$
6.0	$0.00304 \pm 5\text{E-}5$	$0.00369 \pm 3\text{E-}5$	$0.00337 \pm 5\text{E-}4$
8.0	$0.00511 \pm 9\text{E-}5$	$0.00513 \pm 6\text{E-}5$	$0.00512 \pm 2\text{E-}5$
10.1	$0.00889 \pm 2\text{E-}4$	$0.00930 \pm 4\text{E-}5$	$0.00909 \pm 3\text{E-}4$
11.1	$0.0115 \pm 4\text{E-}4$	$0.0119 \pm 2\text{E-}4$	$0.0117 \pm 3\text{E-}4$
12.1	$0.0142 \pm 1\text{E-}3$	$0.0143 \pm 1\text{E-}3$	$0.0142 \pm 6\text{E-}5$



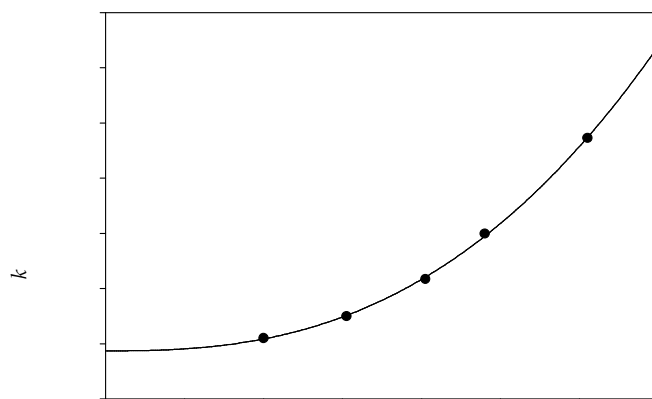
XXXV. Plot of k_{obsd} vs [THF] in 2,2,5,5-tetramethyltetrahydrofuran for the deprotonation of 2-fluoro-3-methylpyridine (**1**, 0.01 M) by LDA (0.20 M) as determined by following loss of **1** at -20 °C. The curve depicts an unweighted least-squares fit to $k_{\text{obsd}} = a + k[\text{THF}]^n$ ($a = 0.541 \pm 0.757$, $k = 0.0150 \pm 0.0163$, $n = 2.75 \pm 0.43$).

[THF] (M)	k_{obsd} (s ⁻¹)
3.9	$0.000948 \pm 5\text{E-}6$
6.0	$0.00267 \pm 4\text{E-}5$
8.0	$0.00565 \pm 7\text{E-}5$
10.1	$0.00877 \pm 1\text{E-}4$
11.1	$0.0112 \pm 2\text{E-}4$
12.1	$0.0151 \pm 5\text{E-}4$



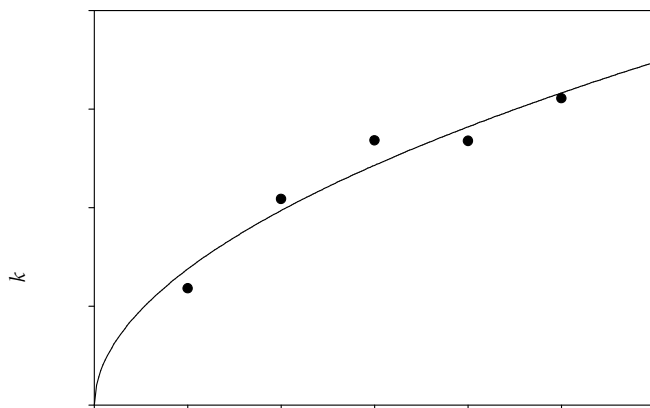
XXXVI. Plot of k_{obsd} vs [LDA] in 4.1 M THF/pentane for the deprotonation of 2-fluoro-3-methylpyridine (**1**, 0.01 M) by LDA as determined by following loss of **1** at $-20\text{ }^{\circ}\text{C}$ by ^{19}F NMR. The curve depicts an unweighted least-squares fit to $k_{\text{obsd}} = k[\text{LDA}]^n$ ($k = 4.90 \pm 0.24$, $n = 0.41 \pm 0.05$).

[LDA] (M)	$k_{\text{obsd}1}$ (s^{-1})	$k_{\text{obsd}2}$ (s^{-1})	$k_{\text{obsd}avg}$ (s^{-1})
0.075	$0.00130 \pm 1\text{E-}5$	$0.00178 \pm 2\text{E-}5$	$0.00154 \pm 3\text{E-}4$
0.15	$0.00187 \pm 2\text{E-}5$	$0.00232 \pm 3\text{E-}5$	$0.00210 \pm 3\text{E-}4$
0.30	$0.00305 \pm 3\text{E-}5$	$0.00365 \pm 3\text{E-}5$	$0.00335 \pm 4\text{E-}4$
0.45	$0.00325 \pm 3\text{E-}5$	$0.00407 \pm 4\text{E-}5$	$0.00366 \pm 6\text{E-}4$
0.60	$0.00394 \pm 5\text{E-}5$	$0.00367 \pm 6\text{E-}5$	$0.00381 \pm 2\text{E-}4$
0.75	$0.00468 \pm 6\text{E-}5$	$0.00386 \pm 6\text{E-}5$	$0.00427 \pm 6\text{E-}4$



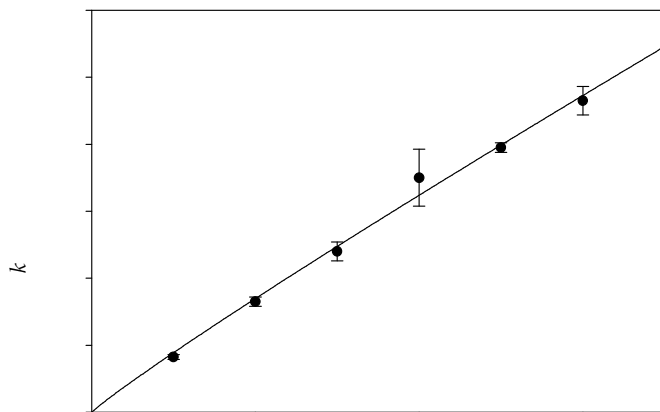
XXXVII. Plot of k_{obsd} vs [THF] in pentane for the deprotonation of 2-fluoro-3-methylpyridine (**1**, 0.01 M) by LDA (0.20 M) as determined by following formation of **5** at -40 °C via in situ IR. The curve depicts an unweighted least-squares fit to $k_{\text{obsd}} = a + k[\text{THF}]^n$ ($a = 1.75 \pm 0.13$, $k = (0.012 \pm 0.003)$, $n = 2.59 \pm 0.11$).

[THF] (M)	k_{obsd} (s ⁻¹)
4.0	$0.000220 \pm 6\text{E-}6$
6.1	$0.000300 \pm 1\text{E-}6$
8.1	$0.000435 \pm 9\text{E-}6$
9.6	$0.000599 \pm 4\text{E-}5$
12.2	$0.000946 \pm 5\text{E-}5$



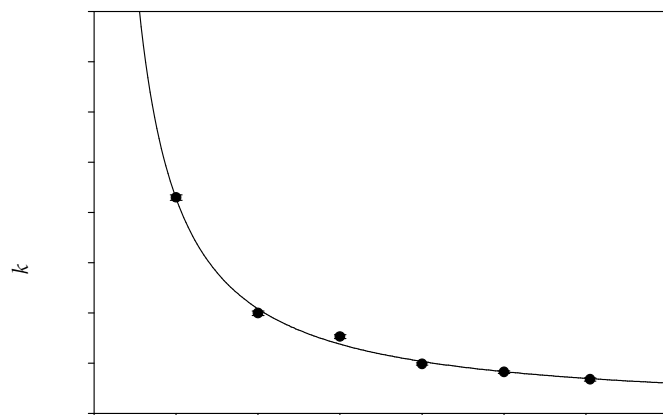
XXXVIII. Plot of k_{obsd} vs [LDA] in 12.3 M THF for the deprotonation of 2-fluoro-3-methylpyridine (**1**, 0.01 M) by LDA as determined by following product formation at -40 °C via in situ IR. The curve depicts an unweighted least-squares fit to $k_{\text{obsd}} = k[\text{LDA}]^n$ ($k = (4.53 \pm 0.47) \times 10^{-3}$, $n = 0.52 \pm 0.09$).

[LDA] (M)	k_{obsd} (s^{-1})
0.10	$0.00118 \pm 7\text{E-}5$
0.20	$0.00209 \pm 2\text{E-}4$
0.30	$0.00268 \pm 2\text{E-}4$
0.40	$0.00268 \pm 2\text{E-}4$
0.50	$0.00311 \pm 3\text{E-}4$



XXXIX. Plot of k_{obsd} vs [LDA] in 10.0 M THF/pentane for the condensation of PhCN (0.01 M) by LDA as determined by following loss of starting material at $-78\text{ }^{\circ}\text{C}$ via in situ IR. The curve depicts an unweighted least-squares fit to $k_{\text{obsd}} = k[\text{LDA}]^n$ ($k = 1.45 \pm 0.24$, $n = 0.93 \pm 0.05$).

[LDA] (M)	$k_{\text{obsd}1}$ (s^{-1})	$k_{\text{obsd}2}$ (s^{-1})	$k_{\text{obsd}avg}$ (s^{-1})
0.05	$0.00085 \pm 2\text{E-}5$	$0.00080 \pm 1\text{E-}5$	$0.00083 \pm 9\text{E-}5$
0.10	$0.0017 \pm 1\text{E-}4$	$0.0016 \pm 1\text{E-}4$	$0.00165 \pm 1\text{E-}4$
0.15	$0.0023 \pm 1\text{E-}4$	$0.0025 \pm 2\text{E-}4$	$0.0024 \pm 1\text{E-}4$
0.20	$0.0038 \pm 2\text{E-}4$	$0.0032 \pm 3\text{E-}4$	$0.0035 \pm 2\text{E-}4$
0.25	$0.0039 \pm 1\text{E-}4$	$0.0040 \pm 1\text{E-}4$	$0.00395 \pm 7\text{E-}5$
0.30	$0.0045 \pm 2\text{E-}4$	$0.0048 \pm 2\text{E-}4$	$0.00465 \pm 8\text{E-}5$



L. Plot of k_{obsd} vs [THF] in pentane for the the condensation of PhCN (0.01 M) by LDA (0.20 M) as determined by following product formation at -78 C via in situ IR. The curve depicts an unweighted least-squares fit to $k_{\text{obsd}} = a + k[\text{THF}]^n$ ($a = 1.76 \pm 0.5$, $k = 0.16 \pm 0.26$, $n = -1.07 \pm 0.07$).

[THF] (M)	$k_{\text{obsd}1}$ (s^{-1})	$k_{\text{obsd}2}$ (s^{-1})	$k_{\text{obsd}avg}$ (s^{-1})
2.0	$0.0085 \pm 3\text{E-}4$	$0.0087 \quad 2\text{E-}4$	$0.0086 \pm 2\text{E-}4$
4.0	$0.0041 \pm 4\text{E-}4$	$0.0039 \quad 3\text{E-}4$	$0.0040 \pm 1\text{E-}4$
6.0	$0.0031 \pm 2\text{E-}4$	$0.0030 \pm 1\text{E-}4$	$0.0031 \pm 1\text{E-}4$
8.0	$0.0019 \pm 1\text{E-}4$	$0.0020 \pm 2\text{E-}4$	$0.00195 \pm 1\text{E-}4$
10.0	$0.0017 \pm 1\text{E-}4$	$0.0016 \pm 4\text{E-}4$	$0.00165 \pm 7\text{E-}5$
12.1	$0.0013 \pm 3\text{E-}4$	$0.0014 \pm 3\text{E-}4$	$0.00135 \pm 9\text{E-}5$

XLI. X-Ray structure of **9**.

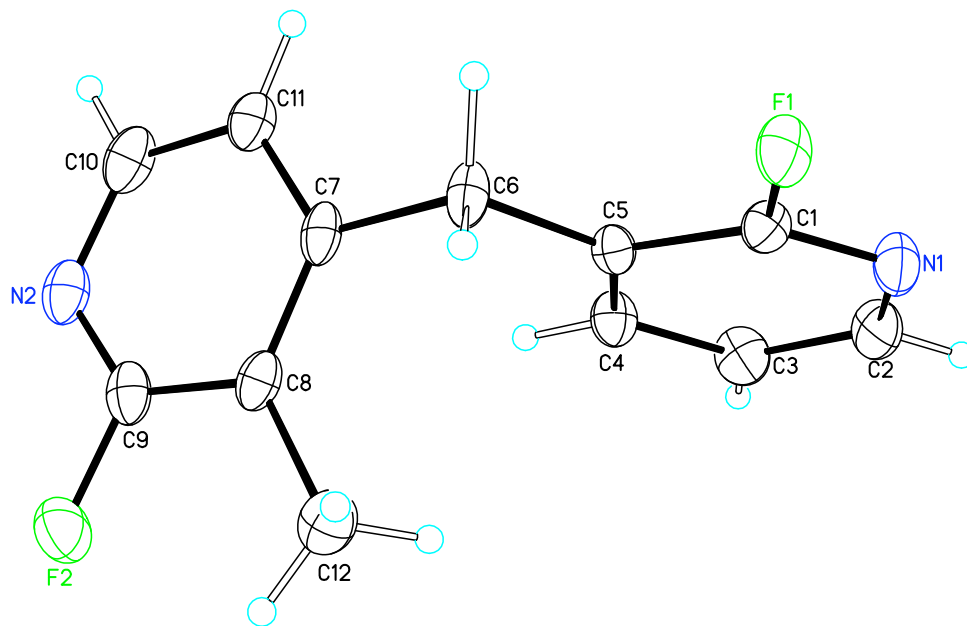


Table 1. Crystal data and structure refinement.

Identification code	9	
Empirical formula	C ₁₂ H ₁₀ F ₂ N ₂	
Formula weight	220.22	
Temperature	173(2) K	
Wavelength	0.71073 Å	
Crystal system	Triclinic	
Space group	P-1	
Unit cell dimensions	a = 7.3370(8) Å	α = 92.050(4)°.
	b = 10.6664(11) Å	β = 95.711(4)°.
	c = 13.1655(14) Å	γ = 94.074(4)°.
Volume	1021.67(19) Å ³	
Z	4	
Density (calculated)	1.432 Mg/m ³	
Absorption coefficient	0.112 mm ⁻¹	
F(000)	456	
Crystal size	0.50 x 0.45 x 0.40 mm ³	
Theta range for data collection	1.56 to 28.49°.	
Index ranges	-9 ≤ h ≤ 9, -14 ≤ k ≤ 13, -17 ≤ l ≤ 17	
Reflections collected	21945	
Independent reflections	5007 [R(int) = 0.0339]	
Completeness to theta = 28.49°	96.7 %	
Absorption correction	Semi-empirical from equivalents	
Max. and min. transmission	0.9565 and 0.9461	
Refinement method	Full-matrix least-squares on F ²	
Data / restraints / parameters	5007 / 0 / 291	
Goodness-of-fit on F ²	1.513	
Final R indices [I > 2σ(I)]	R1 = 0.0767, wR2 = 0.2157	
R indices (all data)	R1 = 0.1012, wR2 = 0.2301	
Largest diff. peak and hole	0.743 and -0.316 e.Å ⁻³	

Table 2. Atomic coordinates ($\times 10^4$) and equivalent isotropic displacement parameters ($\text{\AA}^2 \times 10^3$) $U(\text{eq})$ is defined as one third of the trace of the orthogonalized U^{ij} tensor.

	x	y	z	$U(\text{eq})$
F(1)	1209(1)	1264(1)	8718(1)	33(1)
F(2)	4831(2)	6726(1)	6081(1)	42(1)
F(3)	1972(1)	1148(1)	6266(1)	38(1)
F(4)	-1560(2)	-4333(1)	9015(1)	47(1)
N(1)	3972(2)	505(1)	8843(1)	32(1)
N(2)	4775(2)	7376(1)	7706(1)	33(1)
N(3)	-842(2)	1829(1)	5982(1)	34(1)
N(4)	-1502(2)	-4951(1)	7390(1)	32(1)
C(1)	3050(2)	1482(2)	8695(1)	24(1)
C(2)	5790(3)	694(2)	8810(1)	36(1)
C(3)	6639(2)	1850(2)	8624(1)	34(1)
C(4)	5564(2)	2858(2)	8467(1)	28(1)
C(5)	3691(2)	2710(1)	8506(1)	22(1)
C(6)	2371(2)	3720(1)	8362(1)	28(1)
C(7)	3247(2)	4981(1)	8124(1)	26(1)
C(8)	3699(2)	5217(2)	7153(1)	26(1)
C(9)	4428(2)	6445(2)	7027(1)	29(1)
C(10)	4350(2)	7095(2)	8645(2)	35(1)
C(11)	3595(2)	5943(2)	8894(1)	30(1)
C(12)	3432(3)	4257(2)	6284(1)	36(1)
C(13)	137(2)	895(2)	6236(1)	25(1)
C(14)	-2666(3)	1594(2)	5952(1)	38(1)
C(15)	-3479(2)	451(2)	6172(1)	35(1)
C(16)	-2361(2)	-512(2)	6439(1)	29(1)
C(17)	-490(2)	-306(1)	6479(1)	21(1)
C(18)	872(2)	-1271(1)	6756(1)	26(1)
C(19)	-2(2)	-2542(2)	6992(1)	25(1)
C(20)	-438(2)	-2793(2)	7963(1)	27(1)
C(21)	-1159(2)	-4031(2)	8074(1)	29(1)
C(22)	-1087(2)	-4654(2)	6451(1)	33(1)
C(23)	-342(2)	-3496(2)	6212(1)	27(1)
C(24)	-192(3)	-1867(2)	8844(2)	42(1)

Table 3. Bond lengths [\AA] and angles [$^\circ$].

F(1)-C(1)	1.3577(18)
F(2)-C(9)	1.347(2)
F(3)-C(13)	1.3504(18)
F(4)-C(21)	1.347(2)
N(1)-C(1)	1.292(2)
N(1)-C(2)	1.340(2)
N(2)-C(9)	1.306(2)
N(2)-C(10)	1.344(2)
N(3)-C(13)	1.304(2)
N(3)-C(14)	1.340(2)
N(4)-C(21)	1.301(2)
N(4)-C(22)	1.345(2)
C(1)-C(5)	1.400(2)
C(2)-C(3)	1.383(3)
C(3)-C(4)	1.388(2)
C(4)-C(5)	1.378(2)
C(5)-C(6)	1.503(2)
C(6)-C(7)	1.506(2)
C(7)-C(8)	1.380(2)
C(7)-C(11)	1.407(2)
C(8)-C(9)	1.402(2)
C(8)-C(12)	1.495(2)
C(10)-C(11)	1.376(2)
C(13)-C(17)	1.389(2)
C(14)-C(15)	1.372(3)
C(15)-C(16)	1.393(2)
C(16)-C(17)	1.370(2)
C(17)-C(18)	1.514(2)
C(18)-C(19)	1.514(2)
C(19)-C(20)	1.379(2)
C(19)-C(23)	1.411(2)
C(20)-C(21)	1.406(2)
C(20)-C(24)	1.485(3)
C(22)-C(23)	1.375(2)
C(1)-N(1)-C(2)	115.61(14)
C(9)-N(2)-C(10)	114.15(15)
C(13)-N(3)-C(14)	115.70(15)
C(21)-N(4)-C(22)	114.15(15)
N(1)-C(1)-F(1)	114.56(13)
N(1)-C(1)-C(5)	128.80(15)
F(1)-C(1)-C(5)	116.64(13)
N(1)-C(2)-C(3)	122.73(16)
C(2)-C(3)-C(4)	118.65(16)
C(5)-C(4)-C(3)	120.53(15)

C(4)-C(5)-C(1)	113.67(14)
C(4)-C(5)-C(6)	126.10(14)
C(1)-C(5)-C(6)	120.24(14)
C(5)-C(6)-C(7)	114.32(13)
C(8)-C(7)-C(11)	119.16(15)
C(8)-C(7)-C(6)	120.77(15)
C(11)-C(7)-C(6)	120.06(16)
C(7)-C(8)-C(9)	114.86(15)
C(7)-C(8)-C(12)	123.70(15)
C(9)-C(8)-C(12)	121.44(16)
N(2)-C(9)-F(2)	114.40(14)
N(2)-C(9)-C(8)	128.84(17)
F(2)-C(9)-C(8)	116.76(15)
N(2)-C(10)-C(11)	124.38(16)
C(10)-C(11)-C(7)	118.58(17)
N(3)-C(13)-F(3)	114.99(13)
N(3)-C(13)-C(17)	127.58(15)
F(3)-C(13)-C(17)	117.44(14)
N(3)-C(14)-C(15)	123.12(17)
C(14)-C(15)-C(16)	118.58(17)
C(17)-C(16)-C(15)	119.96(16)
C(16)-C(17)-C(13)	115.06(14)
C(16)-C(17)-C(18)	125.11(14)
C(13)-C(17)-C(18)	119.82(14)
C(19)-C(18)-C(17)	114.19(13)
C(20)-C(19)-C(23)	119.36(15)
C(20)-C(19)-C(18)	121.13(15)
C(23)-C(19)-C(18)	119.49(15)
C(19)-C(20)-C(21)	114.46(15)
C(19)-C(20)-C(24)	124.74(16)
C(21)-C(20)-C(24)	120.80(17)
N(4)-C(21)-F(4)	114.08(14)
N(4)-C(21)-C(20)	129.21(17)
F(4)-C(21)-C(20)	116.71(15)
N(4)-C(22)-C(23)	124.31(16)
C(22)-C(23)-C(19)	118.48(16)

Symmetry transformations used to generate equivalent atoms:

Table 4. Anisotropic displacement parameters ($\text{\AA}^2 \times 10^3$). The anisotropic displacement factor exponent takes the form: $-2\pi^2 [h^2 a^{*2} U^{11} + \dots + 2 h k a^* b^* U^{12}]$

	U11	U22	U33	U23	U13	U12
F(1)	23(1)	24(1)	51(1)	2(1)	6(1)	-6(1)
F(2)	45(1)	38(1)	45(1)	13(1)	10(1)	2(1)
F(3)	26(1)	27(1)	60(1)	10(1)	7(1)	-9(1)
F(4)	54(1)	44(1)	46(1)	12(1)	12(1)	-2(1)
N(1)	33(1)	22(1)	42(1)	6(1)	6(1)	5(1)
N(2)	22(1)	26(1)	50(1)	5(1)	3(1)	4(1)
N(3)	39(1)	26(1)	39(1)	11(1)	8(1)	7(1)
N(4)	21(1)	29(1)	46(1)	7(1)	2(1)	4(1)
C(1)	21(1)	22(1)	28(1)	-1(1)	3(1)	0(1)
C(2)	36(1)	33(1)	44(1)	10(1)	9(1)	18(1)
C(3)	20(1)	40(1)	43(1)	8(1)	4(1)	9(1)
C(4)	23(1)	24(1)	35(1)	4(1)	2(1)	-1(1)
C(5)	21(1)	20(1)	23(1)	2(1)	1(1)	0(1)
C(6)	20(1)	17(1)	48(1)	6(1)	5(1)	2(1)
C(7)	17(1)	19(1)	43(1)	5(1)	1(1)	5(1)
C(8)	19(1)	22(1)	37(1)	0(1)	-1(1)	6(1)
C(9)	18(1)	26(1)	44(1)	9(1)	3(1)	4(1)
C(10)	27(1)	24(1)	51(1)	-6(1)	-3(1)	0(1)
C(11)	26(1)	26(1)	38(1)	1(1)	2(1)	6(1)
C(12)	36(1)	32(1)	39(1)	-2(1)	0(1)	4(1)
C(13)	26(1)	22(1)	27(1)	1(1)	6(1)	-2(1)
C(14)	39(1)	36(1)	40(1)	10(1)	6(1)	15(1)
C(15)	22(1)	41(1)	44(1)	6(1)	4(1)	7(1)
C(16)	22(1)	26(1)	39(1)	4(1)	3(1)	0(1)
C(17)	22(1)	19(1)	21(1)	-2(1)	1(1)	0(1)
C(18)	19(1)	21(1)	39(1)	5(1)	4(1)	-1(1)
C(19)	14(1)	21(1)	41(1)	5(1)	1(1)	3(1)
C(20)	21(1)	25(1)	36(1)	1(1)	1(1)	3(1)
C(21)	19(1)	28(1)	42(1)	10(1)	3(1)	1(1)
C(22)	27(1)	25(1)	44(1)	-4(1)	-3(1)	0(1)
C(23)	21(1)	23(1)	37(1)	2(1)	1(1)	0(1)
C(24)	42(1)	39(1)	44(1)	-5(1)	7(1)	4(1)

Table 5. Hydrogen coordinates ($\times 10^4$) and isotropic displacement parameters ($\text{\AA}^2 \times 10^3$)

	x	y	z	U(eq)
H(2)	6527	4	8919	44
H(3)	7932	1953	8605	40
H(4)	6123	3658	8332	33
H(6A)	1753	3817	8992	34
H(6B)	1416	3443	7798	34
H(10)	4586	7735	9171	42
H(11)	3314	5799	9571	36
H(12A)	4164(9)	3582(8)	6439(2)	54
H(12B)	3780(5)	4630(4)	5685(7)	54
H(12C)	2182(14)	3954(4)	6180(2)	54
H(14)	-3431	2249	5771	45
H(15)	-4778	319	6142	42
H(16)	-2895	-1311	6593	35
H(18A)	1628	-1384	6182	31
H(18B)	1705	-941	7359	31
H(22)	-1325	-5287	5918	39
H(23)	-62	-3341	5536	33
H(24A)	987(15)	-1713(3)	9041(3)	63
H(24B)	-750(7)	-2175(4)	9352(7)	63
H(24C)	-667(7)	-1164(9)	8662(3)	63